ERDC/CHL TR-08-9

Coastal and Hydraulics Laboratory

US Army Corps
of Engineers®
Engineer Research and
Development Center

Southeast Oahu Coastal Hydrodynamic Modeling with ADCIRC and STWAVE

Mary A. Cialone, Mitchell E. Brown, Jane M. Smith,
and Kent K. Hathaway

July 2008

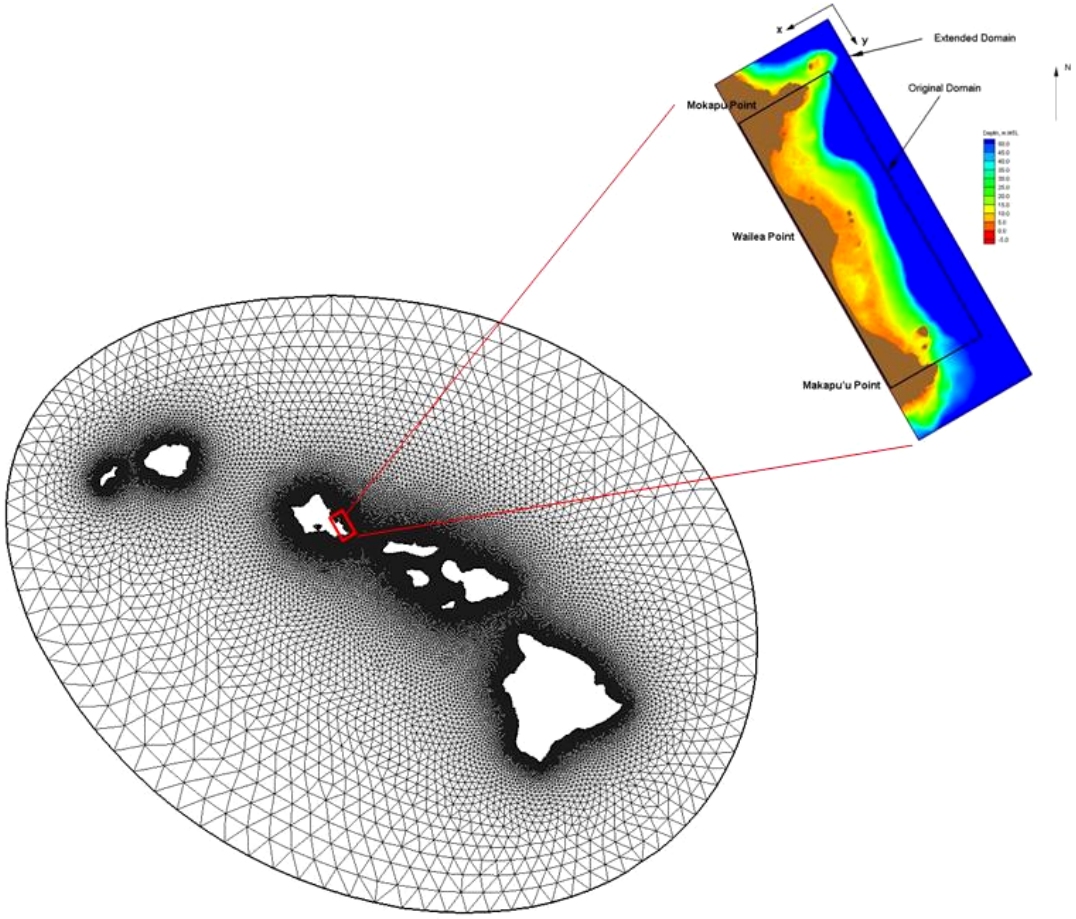

ERDC/CHL TR-08-9
July 2008

Southeast Oahu Coastal Hydrodynamic Modeling with ADCIRC and STWAVE

Mary A. Cialone, Mitchell E. Brown, Jane M. Smith, and Kent K. Hathaway

Coastal and Hydraulics Laboratory
U.S. Army Engineer Research and Development Center
3909 Halls Ferry Road
Vicksburg, MS 39180-6199

Final report

Prepared for U.S. Army Engineer District, Honolulu
Building 230
Fort Shafter, HI 96858-5440

Abstract: This study provides the Honolulu District (POH) with numerical modeling tools for understanding nearshore circulation and sediment transport for Southeast Oahu (SEO). Circulation and wave models are developed and validated for this region and can be applied to assess sediment transport potential for various forcing conditions and to determine the likelihood of accretional and erosional areas within the model domain.

Application of a wave model includes the generation of a wave climate. In the wave climate development technique, nearshore conditions are extracted from the wave model results for each simulation. A transformation correlation between the offshore and nearshore condition is then determined for each simulation. By applying the appropriate transfer function to each wave condition in the offshore time series, a long-term nearshore time series is generated. The nearshore time series demonstrates that there is a reduction in wave height from the offshore location to the nearshore location, landward of the extensive reef system as expected. The technique of developing a nearshore wave climate by applying the wave model for a range of offshore wave conditions provides a permanent "look up" table of nearshore wave conditions at any location in the computational domain and can be applied to any time period for which offshore data are available, provided that bathymetric conditions within the model domain remain similar. POH is applying the database-generated time series to develop sediment transport potential estimates in the project area.

Development of a bottom friction capability in the wave model was completed for application to the extensive reefs in the SEO study area. It is shown that bottom friction is extremely important and has a pronounced effect on modeling transformation over reefs, decreasing wave heights from the without-friction condition by 71-76% for a constant JONSWAP bottom friction value of 0.05.

Contents

Figures and Tables

Figures

Tables

Preface

This technical report describes a hydrodynamic modeling study for Southeast Oahu, Hawaii. The purpose of the nearshore circulation modeling study for the Southeast Oahu Regional Sediment Management (SEO/RSM) demonstration project was for the U.S. Army Engineer Research and Development Center (ERDC), Coastal and Hydraulics Laboratory (CHL) to provide the U.S. Army Engineer District, Honolulu, with a tool for understanding nearshore circulation and sediment transport in the study area. RSM supported field data collection and initial modeling and the Surge and Wave Island Modeling Studies Project supported refinement of STeady-state spectral WAVE model (STWAVE) friction capability and publication of this report. The study was conducted during the period April 2005 through September 2006.

The numerical modeling investigation was conducted by Mary A. Cialone, Coastal Processes Branch (CBP), CHL; and Mitchell E. Brown, Senior Scientist Group, CHL; with technical assistance from Jane M. Smith, CBP, CHL; and data reduction from Dr. Lihwa Lin, Coastal Engineering Branch, CHL. The field data collection was conducted by Kent K. Hathaway, Field Research Facility, CHL; and Raymond Chapman, CBP, CHL; with local assistance from Thomas Smith, Jessica Hays, and Stan Boc, Honolulu District; Chip Fletcher, University of Hawaii at Manoa; and Oliver Vetter, University of Hawaii at Manoa, now of the National Oceanic and Atmospheric Administration.

This project was conducted under the direct supervision of Ty Wamsley, Chief, CPB. General supervision was provided by Dr. William D. Martin, Deputy Director, CHL; and Thomas W. Richardson, Director, CHL.

COL Richard B. Jenkins was Commander and Executive Director of ERDC. Dr. James R. Houston was Director.

1 Introduction

The project area for the hydrodynamic modeling study described in this report is located along the southeast shoreline of the island of Oahu, Hawaii from Mokapu Point to Makapu'u Point (Figure 1). This stretch of coast is considered part of the "windward" side of the island, that is, where the predominant wind travels from the sea to land. Tradewinds and North Pacific waves affect the island's windward side. Tradewind waves occur throughout the year, but are most persistent in the summer, ranging between 1 and 3 m high with periods of 6 to 10 sec. The direction of approach, like the tradewinds themselves, varies between north-northeast and east-southeast and is centered on the east-northeast direction.

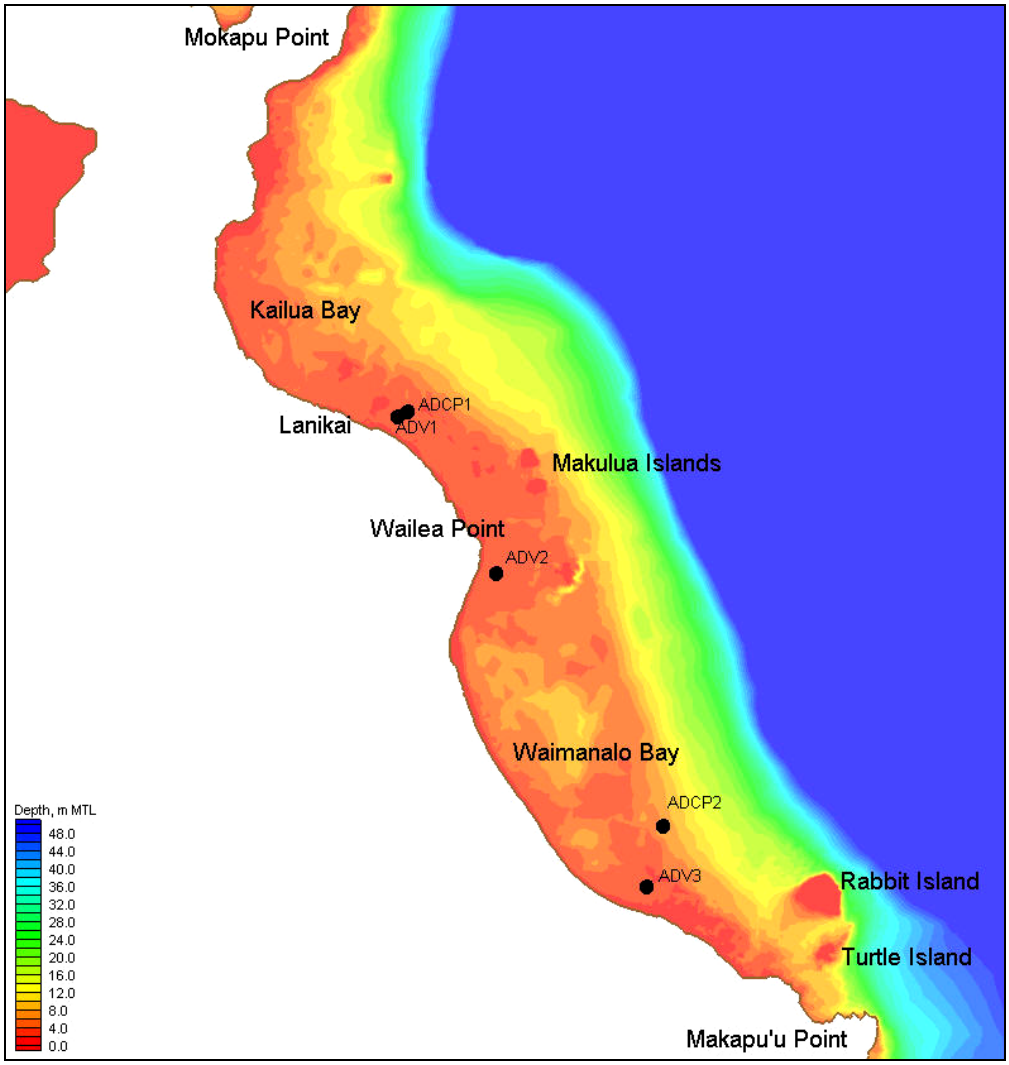

Figure 1. Project area location map and instrument locations.

During the winter months, storms generate large North Pacific swells that range in direction from west-northwest to northeast and arrive at the northern Hawaiian shores with little attenuation of wave energy. Deep-water wave heights often reach 5 m and, in extreme cases, can reach 9 m with periods of 12 to 20 sec. In the study area, offshore waves are generally from the east-northeast and range in height from 0.5 to 6.0 m. Peak wave periods are generally 6 to 16 sec (Sea Engineering 2008).

The ultimate goal for the Honolulu District (POH) was to understand sediment transport potential in the region and determine the likelihood of accretional and erosional areas within the model domain. There are three littoral cells along the project reach: Kailua in the north, Lanikai in the central portion, and Waimanalo in the southern part of the study area in which geologic controls (both subaerial and offshore) affect sediment transport. The offshore region is a sloping reef along which depth-limited waves break. Long-term (decadal or longer) shifts in wind, wave direction, and wave period have the potential to shift sediment transport patterns and magnitudes, therefore making sediment transport processes for this region difficult to understand. The focus of the work presented in this report, however, is the nearshore circulation study project, which included six technical tasks:

1. data collection/assessment,
2. finite-element and finite-difference grid development,
3. development of model forcing conditions,
4. model validation,
5. model simulations, and
6. simulation analysis.

The final product from these tasks was validated hydrodynamic and wave models for the Southeast Oahu (SEO) region. The Honolulu District could then apply the models with various forcing conditions to achieve their goal in better understanding the nearshore circulation and sediment transport potential in the region and determining the likelihood of accretional and erosional areas within the model domain.

Circulation (ADCIRC) and wave (STWAVE) models were applied in this study. The ADvanced CIRCulation (ADCIRC) long-wave hydrodynamic model simulates the circulation and water levels associated with both tides and atmospheric conditions (Luettich et al. 1992).

The two-dimensional, depth-averaged version of ADCIRC was applied in this study. ADCIRC has been extensively applied in the Atlantic and Pacific Oceans (and world wide) to simulate tidal circulation and associated storm surge and currents (U.S. Army Corps of Engineers (USACE) 2006; USACE, Mobile District, 2008; Kraus and Arden 2003; Kraus 2006). The hydrodynamic modeling component for this study required:

1. grid development to include recent bathymetry and shoreline data,
2. validation of the bathymetric grid to known tidal constituents and wind forcing, and
3. comparison of the ADCIRC simulation model results for the bathymetric grid forced with known tidal constituents, wind, and waves to measurements for the field data collection time period.

The application and validation of ADCIRC for the SEO study provides POH with the capability of simulating circulation in the study area for any required time period.

The STeady-state spectral WAVE model (STWAVE) is a spectral wave transformation model, which is capable of representing depth-induced wave refraction and shoaling, current-induced refraction and shoaling, depth- and steepness-induced wave breaking, diffraction, wind-wave growth, wave-wave interaction and whitecapping (Resio 1988; Smith et al. 2001). The purpose of applying nearshore wave transformation models such as STWAVE is to describe quantitatively the change in wave parameters between the offshore and the nearshore. Offshore time-series wave data are typically available; however, nearshore wave information is required for the design of almost all coastal engineering projects. STWAVE has previously been applied to numerous sites with a gently sloping seafloor or small areas of hardbottom. Due to the wide and relatively shallow reef fronting the shoreline of the SEO region, this application of STWAVE required the added feature of simulating wave transformation over a reef. Development of a bottom friction capability in STWAVE was completed to address this unique bathymetry specific to the island environment. Application of STWAVE for this project required development of a computational grid to simulate wave propagation, verification of calculated waves by comparison to measurements, and generation of a wave climate. The ADCIRC and STWAVE models were then coupled to allow the STWAVE radiation stresses to force circulation within ADCIRC.

The approach toward development of a "turn-key" hydrodynamic modeling system for this region was pursued in a phased process. In the first phase, the Honolulu District and the Coastal and Hydraulics Laboratory (CHL) jointly developed the geographic, bathymetric, hydrodynamic (waves and circulation), and meteorological data necessary to develop and validate the modeling system. An assessment of the quality of available data aided in the specification of additional field measurements that were to be collected for this project. CHL developed and validated the ADCIRC model for tidal constituent forcing at the ocean boundary condition using the Oregon State University (OSU) Pacific constituent database. Development of the finite-element grid for the overall project focused on a coarse resolution at the seaward, deepwater boundaries and detailed resolution in the nearshore region of interest. All recently collected bathymetric data, including SHOALS (Wozencraft and Irish 2000) data collected in 2000, were evaluated and incorporated into the model grid, and bathymetric databases were used to supplement bathymetry for the grid domain.

In Phase 2 development, CHL established the range of atmospheric forcing required for accurate simulations. CHL developed the STWAVE grid, validated the STWAVE model, and performed an additional ADCIRC validation including atmospheric forcing and coupling with STWAVE. These validation simulations utilized the field measurement effort for comparison to model results. Tidal forcing conditions were developed for the ocean boundary condition with the LeProvost tidal constituent database, which provided a stable solution for the linked model validation time period (LeProvost et al. 1994). Offshore wind and pressure fields generated by a combination of wind fields and pressures adjusted for local observations were used as forcing conditions for the hydrodynamic model. These fields are discussed in detail in Chapter 3, section on "Wind sources." Wave conditions from a Coastal Data Information Program (CDIP) buoy near the study site were used to generate boundary forcing conditions for the wave model. STWAVE was validated by comparing model-predicted and field measurements of wave conditions at the field data collection locations. The bottom friction was calibrated in the model to represent the reef and non-reef areas until a close comparison was achieved. ADCIRC was validated by comparing model-predicted and field measurements of water level and velocity at the field data collection locations. A hybrid friction formulation in ADCIRC and a range of wave radiation stress gradients from STWAVE were applied to achieve the best comparison.

In Phase 3, CHL assisted POH in developing recommendations for alternative simulations, documented the methodologies and procedures, and provided consultation in executing simulations and analyzing simulation results. The completed modeling system has been transferred to the Honolulu District within the Surface Water Modeling System (SMS) framework and training has been provided to the Honolulu District for future applications.

2 Field Data Collection

Wave and current data were collected for this project from 9 August to 14 September 2005 with two RD Instruments Workhorse Acoustic Doppler Current Profilers (ADCPs) and three Sontek Hydra Acoustic Doppler Velocimeters (ADVs). The field data collection deployment period was dominated by tradewind weather (typically occurring from April through September in Hawaii) as characterized by consistent winds from the northeast and occasional swells from the southeast and southwest. Large wave events affecting the windward coast are not typical during this season. Waves along the windward coast during these months are typically generated from local winds, and this is evident in the relatively small wave heights and northeasterly incident direction of the waves recorded during the deployment period. Instrument locations and additional information are shown in Figure 1 and Table 1. All recording gauges were referenced to coordinated universal time (UTC).

Table 1. Instrument identification and location (Hawaii RSM gauge locations, August–September 2005).

Gauge		Latitude deg min	Longitude deg min	Recording Time Period	Nominal Depth, m
Type	Name				
ADCP	ADCP1	21 23.905	157 42.994	9 August–14 September	3.3
ADCP	ADCP2	21 20.318	157 40.786	10 August–4 September	6.6
ADV	ADV1	21 23.861	157.43.079	9 August–14 September	2.5
ADV	ADV2	21 22.509	157 42.233	9 August–14 September	2.7
ADV	ADV3	21 19.795	157 40.930	9 August–14 September	2.5

ADCP gauges

For this study, two RD Instruments 1200 kHz Workhorse ADCP gauges were deployed for approximately 1 month. The ADCPs were bottom mounted, facing upward with the sensor head approximately 0.4 m off the bottom. The water depth at ADCP1 was approximately 3.3 m and the water depth at ADCP2 was approximately 6.6 m, located near the seaward edge of the reef flat. These gauges have four acoustic transducers for measuring currents and a pressure sensor, from which horizontal and vertical current profiles were computed at 0.2 m vertical spacing. Waves were calculated from the decay in orbital velocities. These instruments sampled at 2 Hz for

directional wave measurements. Each hourly wave burst was approximately 34 min long, starting at the top of each hour, and consisted of 4096 points. The instruments have a 0.44-m blanking distance from the transducer head, and a 0.2-m bin width makes the first sample 0.72 m above the transducer. The profiles, therefore, span from 1.12 m off the ocean bed to the moving free surface position. Current profiles were collected every 10 min from a 200 point average.

The ADCP deployments were on 9 August 2005 and retrieval was on 14 September 2005. ADCP2 was reprogrammed on 10 August so data collection started a day later than the other instruments, and the batteries were depleted on 4 September, about 10 days before retrieval of all gauges. The ADCP2 data record was, therefore, 11 days shorter than the other gauge records.

ADV gauges

In addition to the two ADCPs, three ADV gauges were deployed for the same 1-month time period. ADV deployments were on 9 August 2005 and retrieval was on 14 September 2005. The three ADV gauges were Sontek's Hydra model that samples a single-point current velocity (U, V, and W) and contains an external pressure sensor. With these instruments, wave height, period, and direction are determined from PUV analysis (pressure and orbital velocities) (Guza and Thornton 1980). The sample volume for the current measurement is approximately 1–2 cm in size and about 0.17 m above the center transducer. This instrument uses three beams to determine the three current components. Both the ADCP and ADV instruments and their mounts are shown in Figure 2. Figure 3 shows wave height, peak period, and mean direction for the three ADV gauges. Figure 4 depicts wave roses (peak direction) for the two ADCP gauges.

Current drogues

Four current drogues (drifters) were designed and built at the CHL Field Research Facility (FRF) in Duck, NC, for deployment at the beginning (10 August 2005) and end (13 September 2005) of the ADCP/ADV deployment period. The approximately 1-m by 1-m drogues were constructed with polyvinyl chloride (PVC) pipe, vertical risers, rubber unions (connectors), hose clamps, and sails. They used Global Positioning System (GPS) receivers for tracking and radio telemetry for positioning (Figure 5).

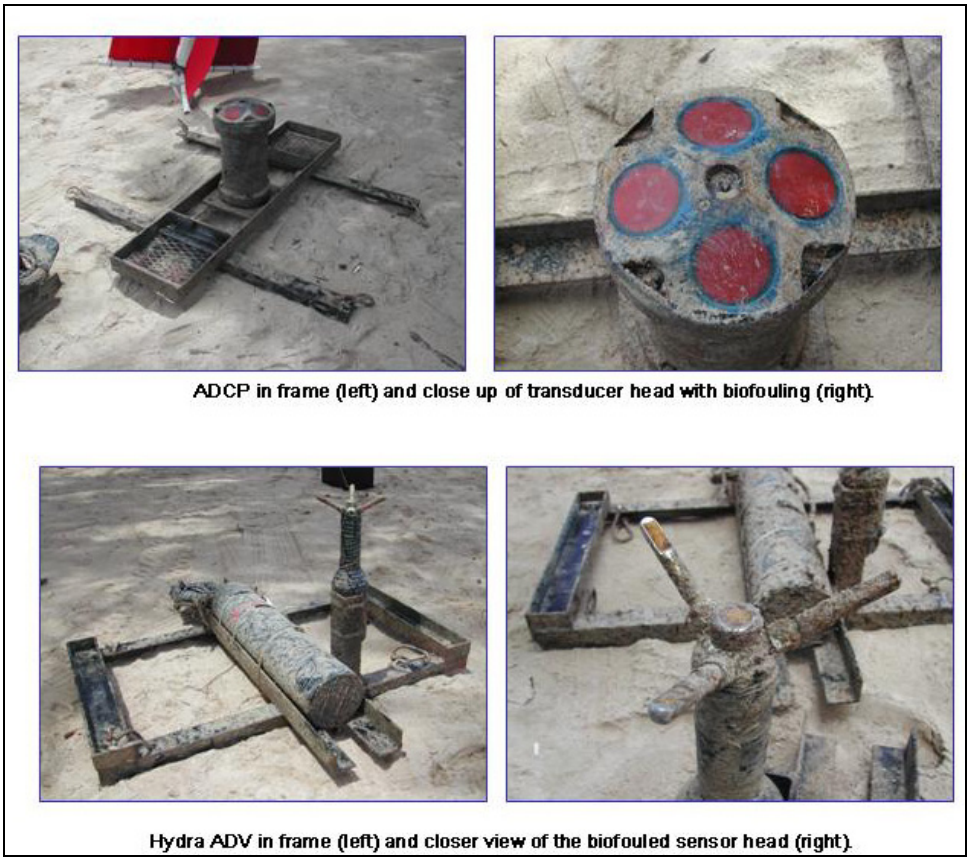

Figure 2. Images of gauges and mounts.

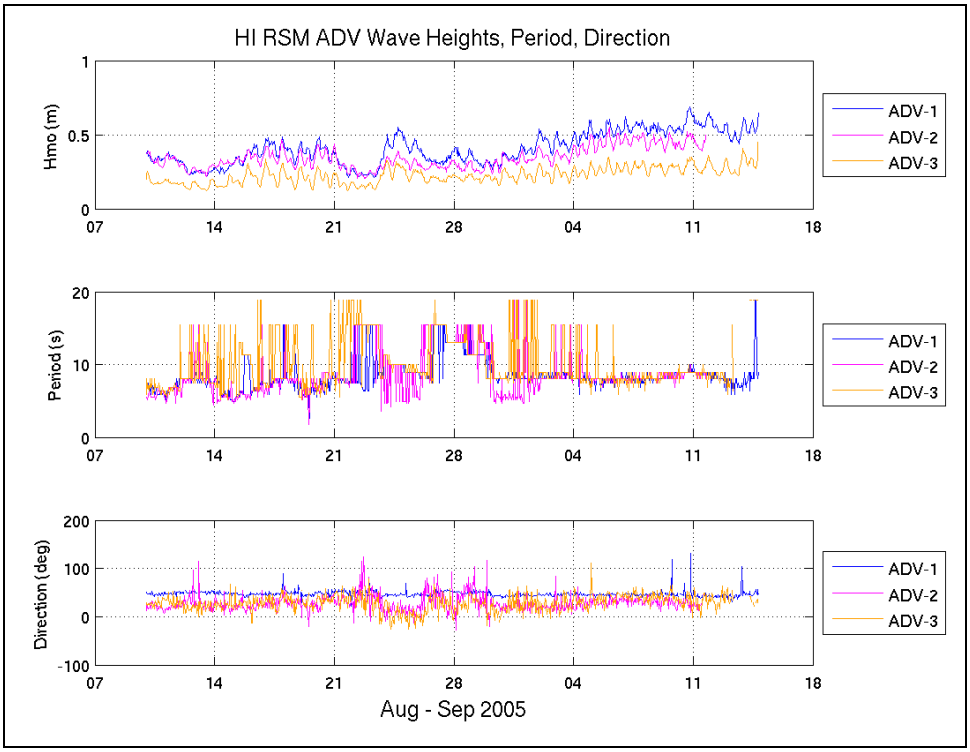

Figure 3. Wave height, period, and direction from the three ADV gauges.

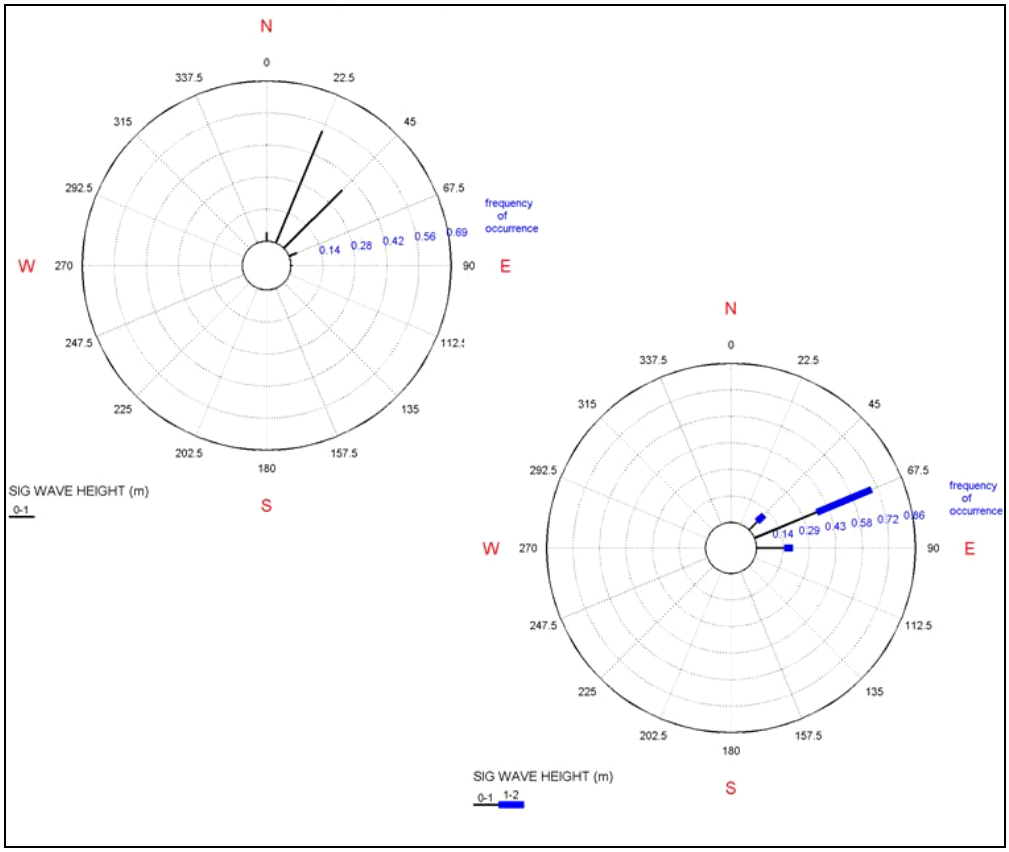

Figure 4. Wave roses for ADCP #1 (left) and #2 (right).

Figure 5. GPS current drogue (left) with traditional drifter (behind grapefruit) and Hawaiian drifter (coconut). Drifter floats just below surface (right).

The drogues floated just below the surface, which placed the bottom of the sail about 1 m from the ocean surface. Difficulty with the radio tracking was experienced because it required line of sight to receive signals from the drifters. Since the drifters were in two different locations (Kailua Bay and Waimanalo Bay), partial tracking was all that could be accomplished. In addition, two antennas and connectors were broken during deployment.

Current drogue tracks for 10 August 2005 and 13 September 2005 are shown in Figure 6. There were two deployments on 10 August, hence the numbers 1 through 8. Some drogues were deployed in the vicinity of the ADV and ADCP gauges for inter-comparison. A track direction reversal of Drogue #2 was observed shortly after deployment on 13 September (Figure 7), starting off on a nearly due west track and then turning back to a southeast trajectory. The nearshore drogues tended to track in a westerly (shoreward) direction at a rate of approximately 0.1–0.2 m/sec, which is comparable to model results. Drogues in Waimanalo Bay moved in a southerly direction during the two deployment periods.

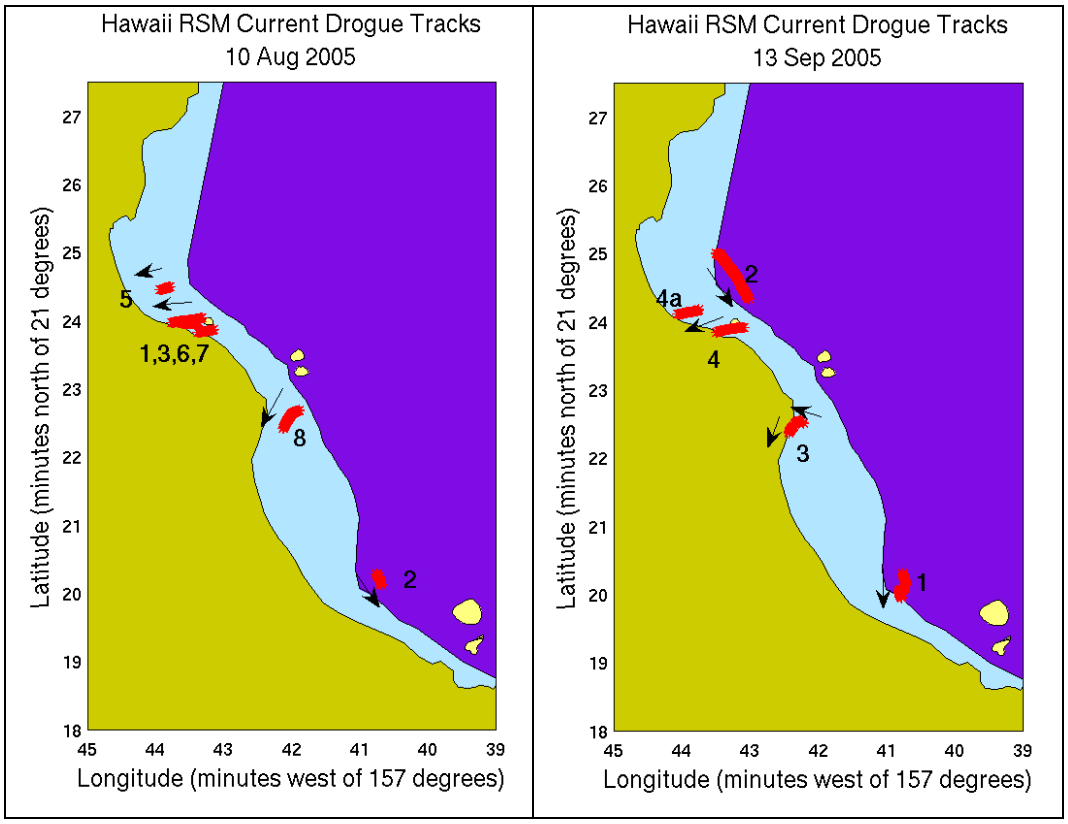

Figure 6. Drogue tracks with track numbers for 10 August (left) and 13 September (right).

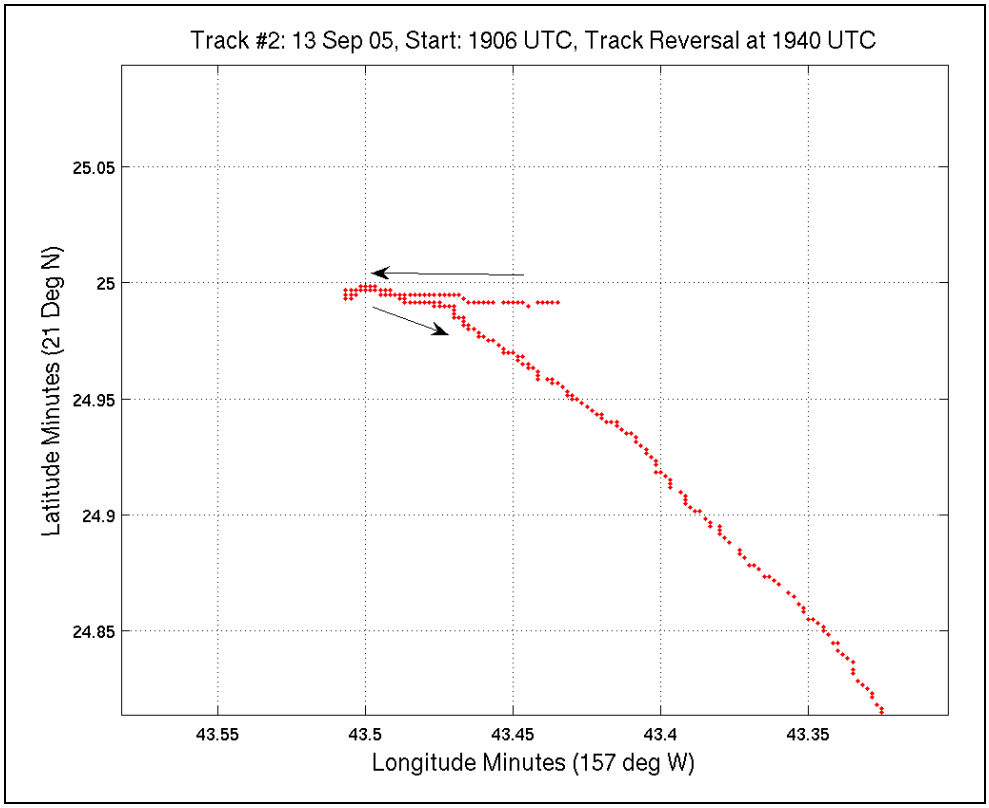

Figure 7. Drogue track reversal on 13 September.

3 Hydrodynamic Modeling

ADCIRC grid development

The ADCIRC (Luettich et al. 1992) numerical model, a regional two-dimensional (2-D) depth-integrated, finite-element hydrodynamic circulation model, was applied in this study to provide water level and depth-averaged current (circulation) information for SEO. The model solves the shallow-water equations in full nonlinear form and can be forced with tide, wind, waves, and flux boundary conditions. Two ADCIRC model grids were developed in the course of this modeling initiative. The first grid was a large circular grid centered on the SEO region and extended from the central point approximately 21 degrees latitude and longitude (2,300 km) in all directions. Initial attempts at validation were unsuccessful because of the existence of two tidal amphidromes that were close to the forcing boundary, shown in Figure 8. (An amphidrome is a location in the ocean where tidal amplitude is zero due to canceling of tidal waves.) To eliminate the problem introduced by the tidal amphidromes, the spatial extent of the ADCIRC model domain was reduced.

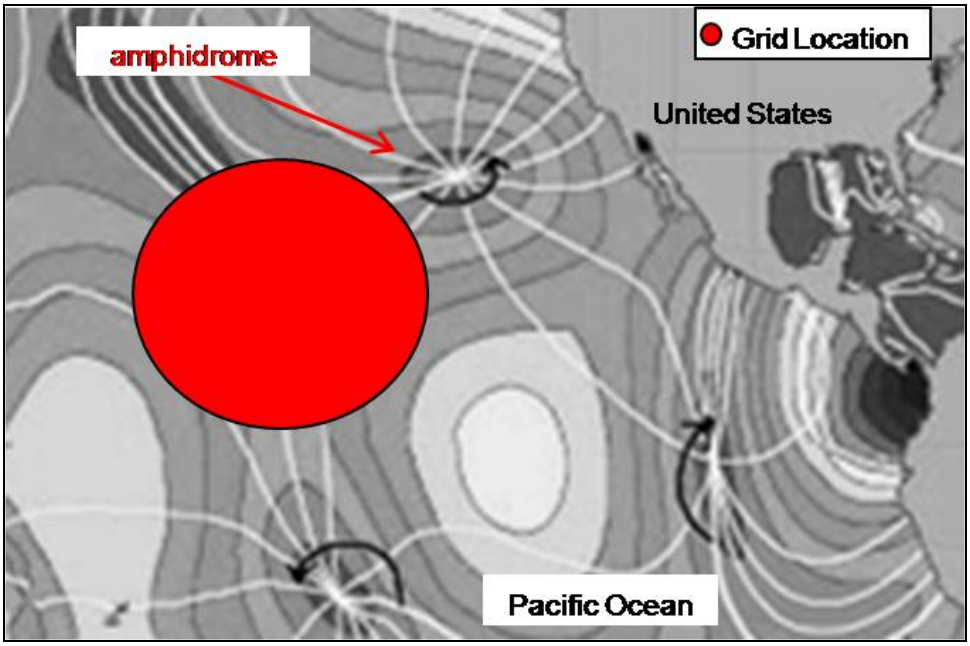

Figure 8. Approximate location of grid and amphidrome locations (background image from http://en.wikipedia.org/wiki/Image:M2_tidal_constituent.jpg).

The final ADCIRC mesh, shown in Figure 9, was a subdomain of the initial grid and is oblong in shape due to the orientation of the Hawaiian Islands. Depths on the mesh were referenced to mean tide level (mtl). The mesh contains 73,305 computational nodes and 140,849 elements. Individual element area ranges from a maximum of 462,500 km² in deep water to a minimum of 60 m² surrounding many of the island features. High resolution was added to the existing ADCIRC mesh in the study area around bathymetric features, such as islands, entrances, and reefs. The refined grid had many improvements over the initial grid:

1. The ADCIRC grid mesh is forced with the free surface position along the open-water boundary that surrounds the Hawaiian Islands. Since the extent of the grid domain for the final grid is smaller than the grid extent for the initial grid, the forcing boundary for the final grid is far away from the influence of the tidal amphidromes shown in Figure 8.
2. The area of Honolulu Harbor is better resolved in the final grid, which improves the comparison between calculated tides and gauge data in this area.

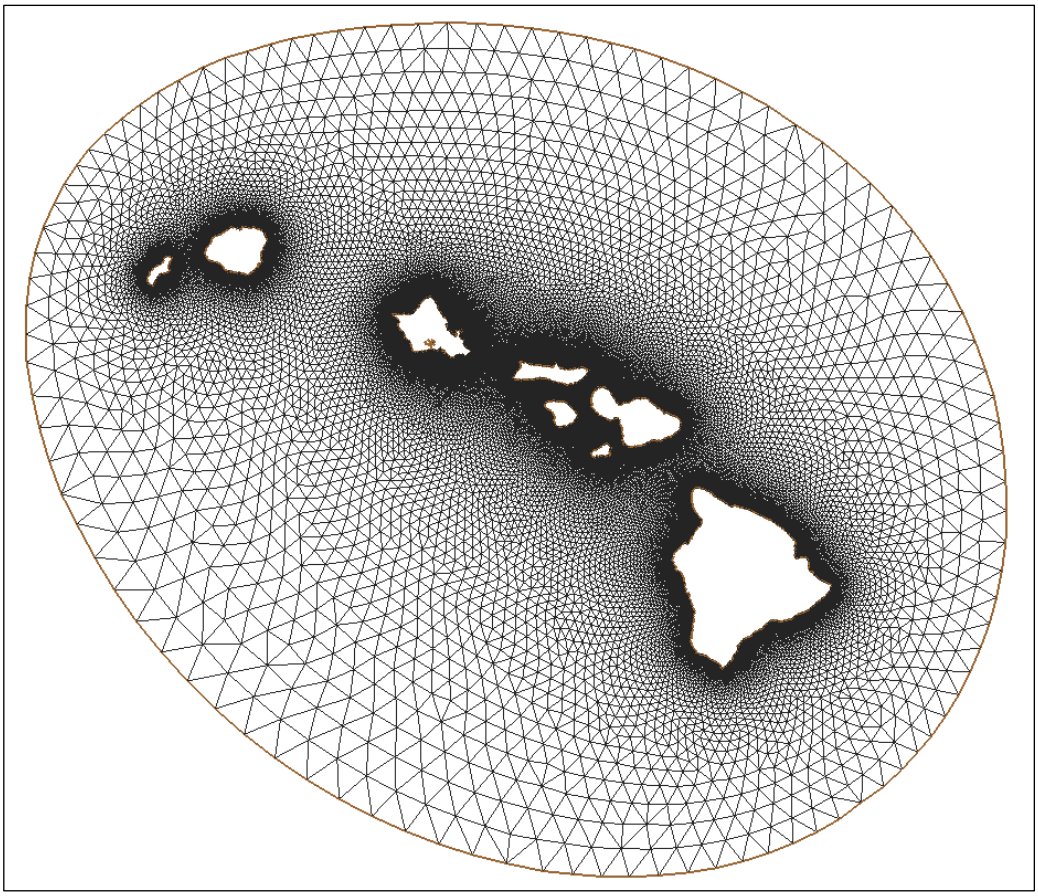

Figure 9. Final ADCIRC mesh domain.

3. Resolution around prominent features in the project reach was added, as well as topographic information for Rabbit and Turtle Islands located in the southern portion of the SEO region.

Wind sources

Three wind sources were investigated for potential application as a forcing condition in the ADCIRC model: National Oceanic and Atmospheric Administration (NOAA) National Data Buoy Center (NDBC) Buoy 51001, National Centers for Environmental Prediction (NCEP) hindcast, and Oceanweather, Inc. (OWI) hindcast wind data. The elevation of NCEP and OWI wind sources was 10 m. The NDBC buoy data were empirically transformed from the 5-m to 10-m elevation. A comparison of the observed (transformed) wind speed and direction at the NDBC Buoy 51001 and the nearest NCEP prediction point was performed for the months of January to June 2001 (Figure 10). Wind directions compared well; however, the NCEP wind speed consistently exceeded the buoy observations by 5 to 10 percent. These differences can be attributed to the buoy anemometer height being empirically transformed from the 5-m to 10-m elevation, whereas the NCEP surface level winds are predicted at an elevation of approximately 10 m. The comparisons suggest that long-term, historic NCEP winds can be applied in this project with a high degree of confidence for the initial validation time period.

NDBC Buoy 51001 winds were also compared to the predicted OWI basin level Pacific hindcast winds for the month of April 2001. A plot of this comparison is shown in Figure 11. Wind speed and directions compared well. These data suggest that OWI winds can also be applied to the project with a high degree of confidence. OWI winds were applied for the second validation (gauge deployment) time period.

ADCIRC model validation – wind and tide for initial validation time period

In the initial validation, the time period 10–24 April 2001 was selected for comparing model results to measured data because the OWI winds compared well with other wind sources for this time period. ADCIRC was forced along the open boundary with tidal information extracted from the OSU TOPEX/POSEIDON Crossover (TPXO) tidal database (Egbert et al. 1994). Wind speed and direction information were obtained from NDBC Buoy 51001. The ADCIRC hydrodynamic time-step was 0.4 sec and results

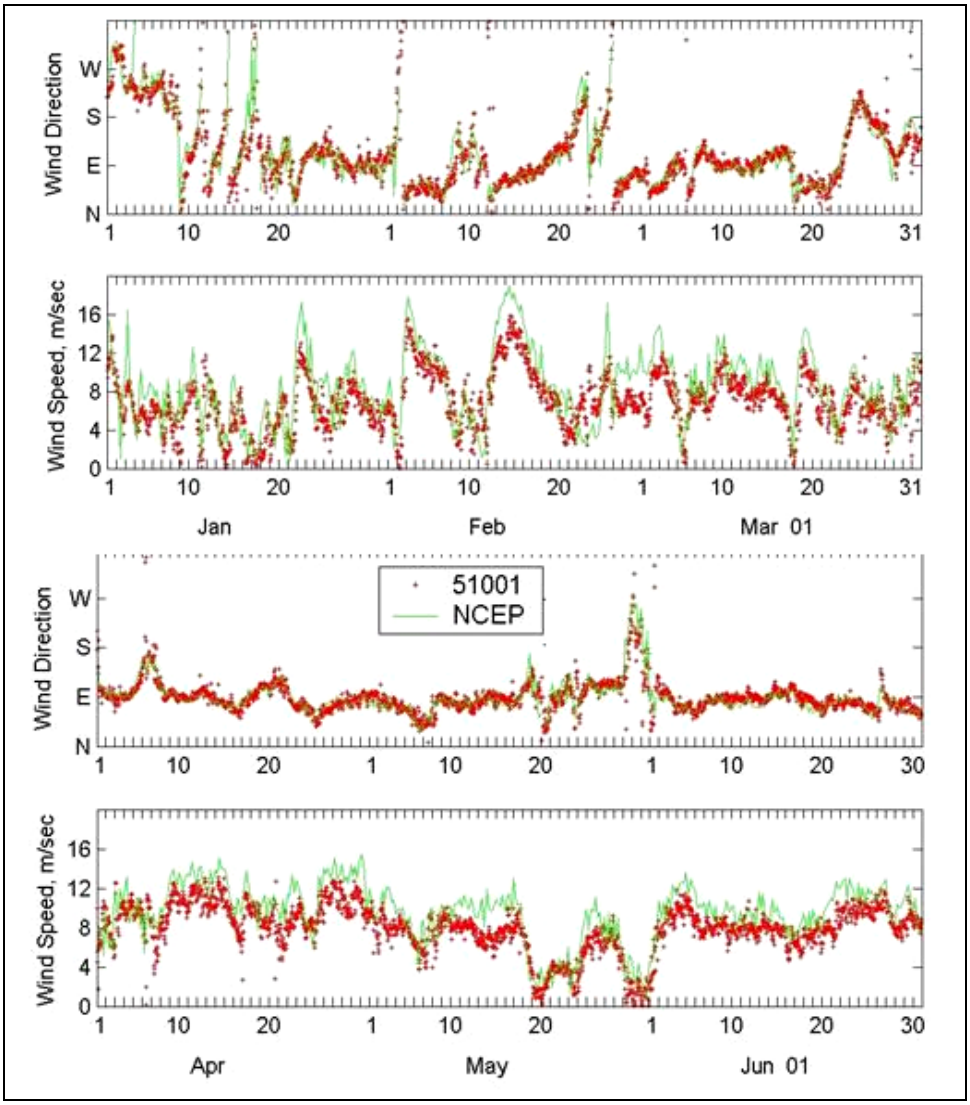

Figure 10. Comparison of observed (NDBC Buoy 51001) transformed to the 10-m elevation and predicted (NCEP) wind speed and direction.

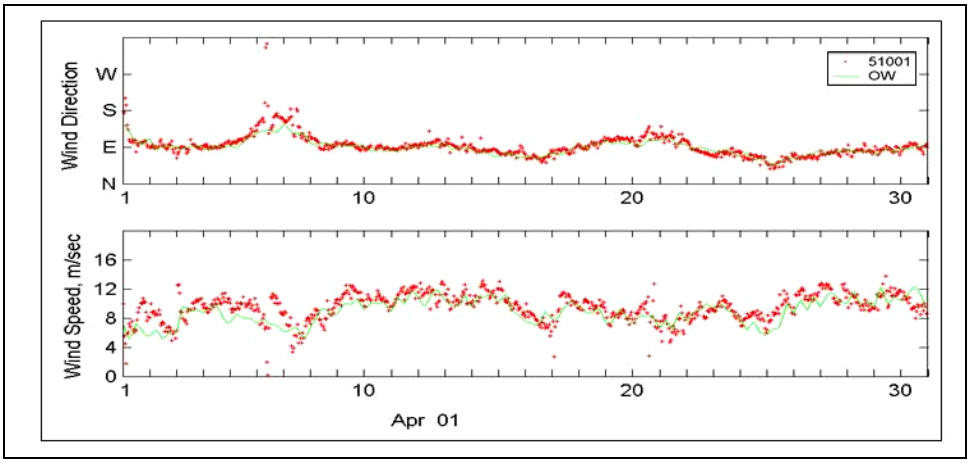

Figure 11. Comparison of observed (NDBC Buoy 51001) and predicted (OWI) wind speed and direction for April 2001.

were reported hourly. Simulations were performed on the U.S. Army Engineer Research and Development Center's (ERDC) High-Performance Computer (HPC) system in Vicksburg, MS, due to the large size of the ADCIRC domain.

For this initial model validation, ADCIRC results for water level were compared with the two NOAA tide gauges available on the southern and eastern portion of the island of Oahu. Figure 12 shows the locations of the two gauges (red circles) and their proximity to the project area (black box). The calculated water levels from the ADCIRC simulation of the April 2001 time period compared relatively well in range and phase with the NOAA gauge measurements, considering that the locations of the gauges were well outside the area of high resolution in the project area. Water level comparisons of the ADCIRC validations to the two NOAA gauges, Honolulu Harbor and Kaneohe Bay, are shown in Figures 13 and 14. Since these gauges were outside the project area and located in less resolved locations, it was determined that another validation would be made with the water level and current data received from ADV and ADCP gauges for the deployment period from 10–31 August 2005. Results of that validation are provided later in section entitled, "ADCIRC validation—wind, tide, and waves for gauge deployment time period."

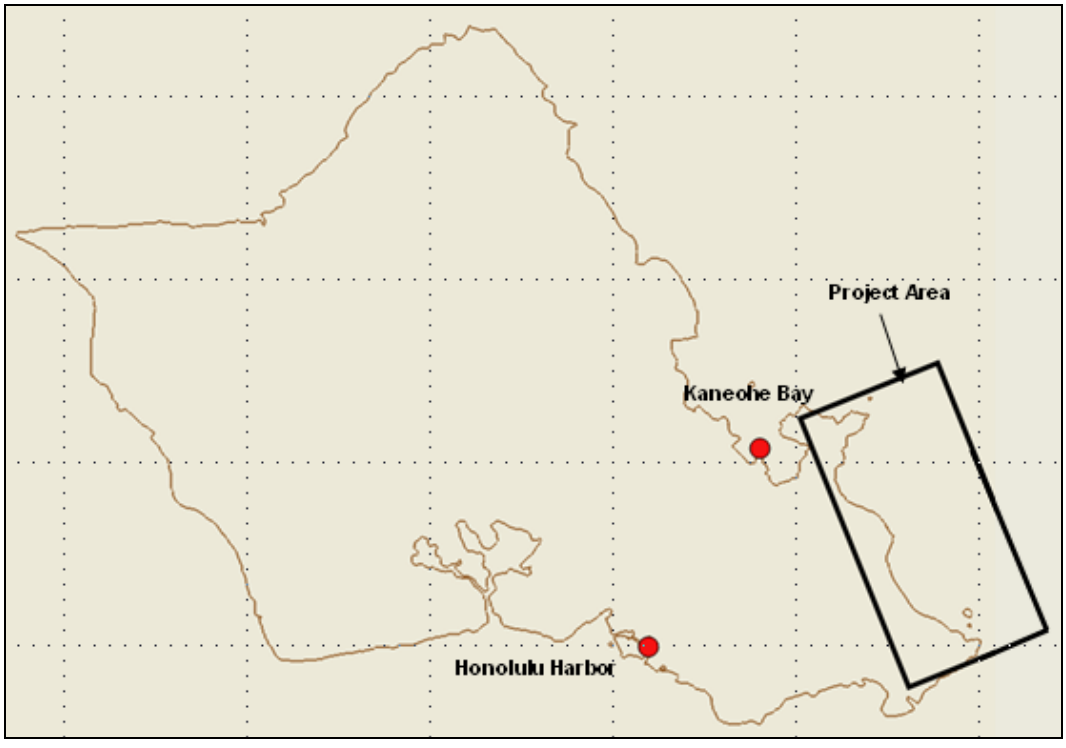

Figure 12. NOAA gauge locations for initial validation time period.

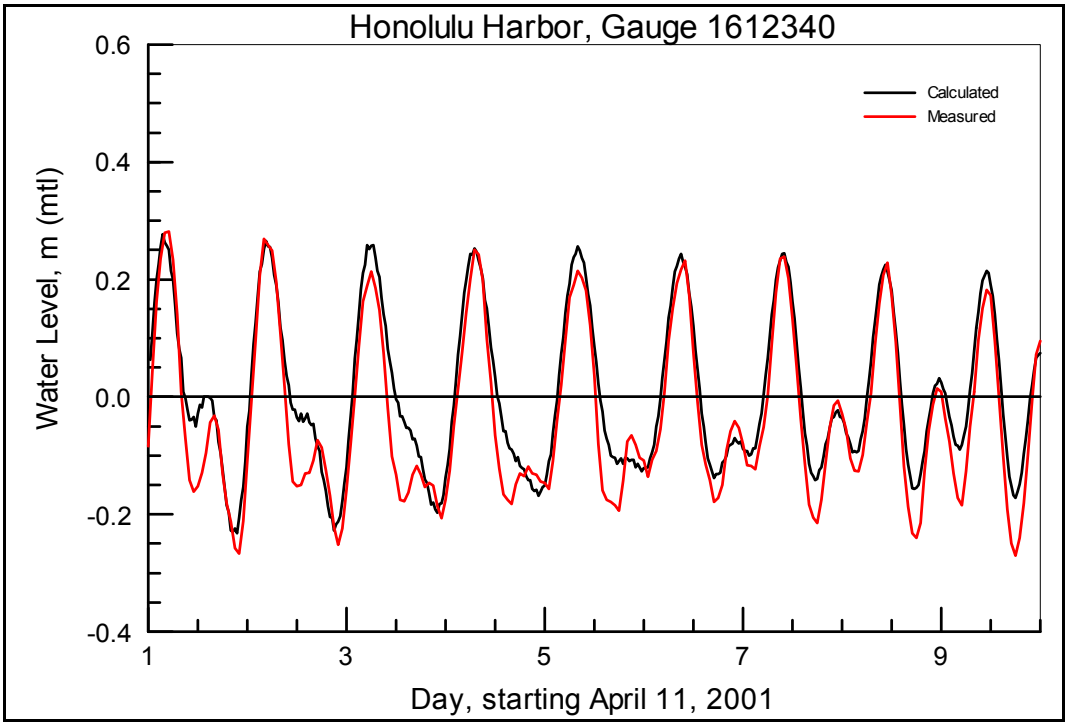

Figure 13. Comparison of calculated and measured water level at Honolulu Harbor gauge for initial validation period.

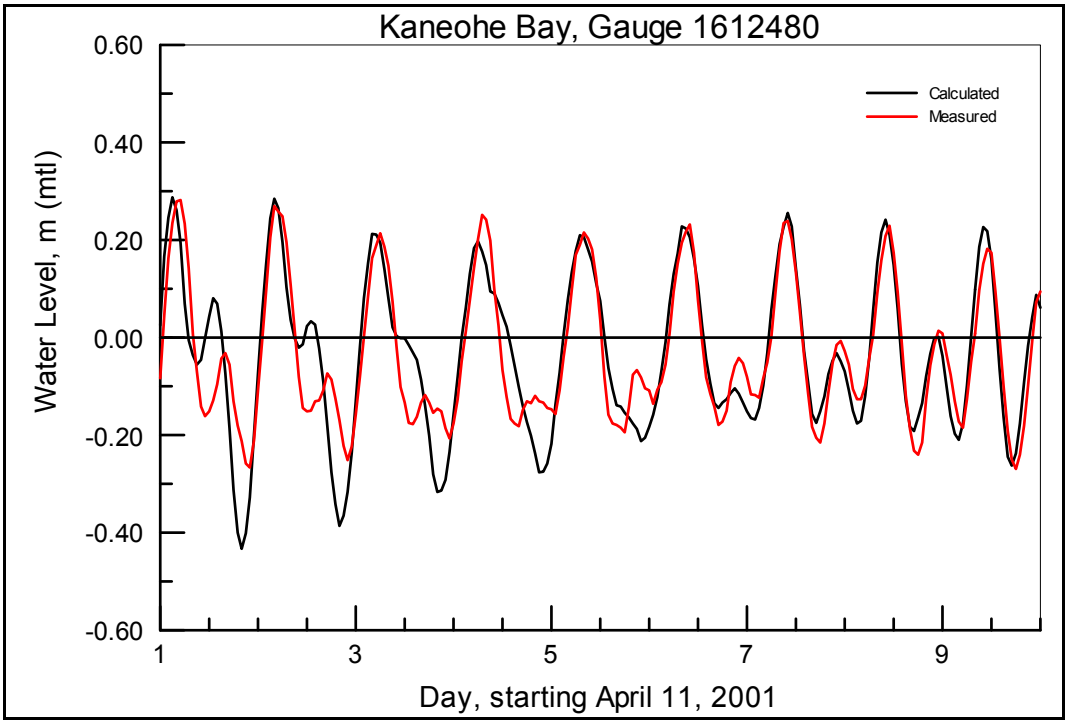

Figure 14. Comparison of calculated and measured water level at Kaneohe Bay gauge for initial validation period.

STWAVE

STWAVE is a steady-state, finite-difference model based on the wave action balance equation (Resio 1988; Smith et al. 2001). STWAVE simulates depth-induced wave refraction and shoaling, current-induced refraction and shoaling, depth- and steepness-induced wave breaking, diffraction, wind-wave growth, wave-wave interaction, and white-capping. The purpose of applying nearshore wave transformation models is to quantitatively describe the change in wave parameters between the offshore and the nearshore and, in this application, include simulating wave transformation over a reef. As previously mentioned, development of a spatially varying bottom friction capability in STWAVE was completed to enable application to the extensive reefs in the SEO study area.

Grid development

An STWAVE finite-difference grid was developed for the study area, with bathymetry interpolated from the ADCIRC grid mesh. The STWAVE grid resolution was 25 m × 25 m with a grid orientation of 210 deg counterclockwise from east. The original grid was 18 km (720 cells) in the alongshore direction by 6.2 km (248 cells) in the cross-shore direction and extended in the offshore to approximately the 100-m contour, with a maximum 344 m depth (Figure 15). After initial testing and consultation with the Honolulu District, it was determined that the lateral extent of the grid should be expanded around the headlands and the offshore boundary should be extended beyond the shallow water offshore from Mokapu Point and Makapu'u Point. The extended grid was 24.2 km (968 cells) in the alongshore direction by 7.8 km (310 cells) in the cross-shore direction and extended in the offshore to approximately the 300-m contour, with a maximum 480-m depth (Figure 15). The initial grid was applied for wave climate development and nearshore database generation. The extended grid was applied for comparison to field data and linkage to the ADCIRC model.

Wave climate -- model forcing conditions

Directional wave data were available at CDIP Station 098 (Mokapu Point) from August 2000 through 2004 (the study started in March 2005). Nondirectional wave data were available at Station 034 (Makapu'u) from 1981 to 1996. Directional wave data were available for Station 099 (Kailua Bay) for 2 months (November–December 2000). Station locations are shown in Figure 16.

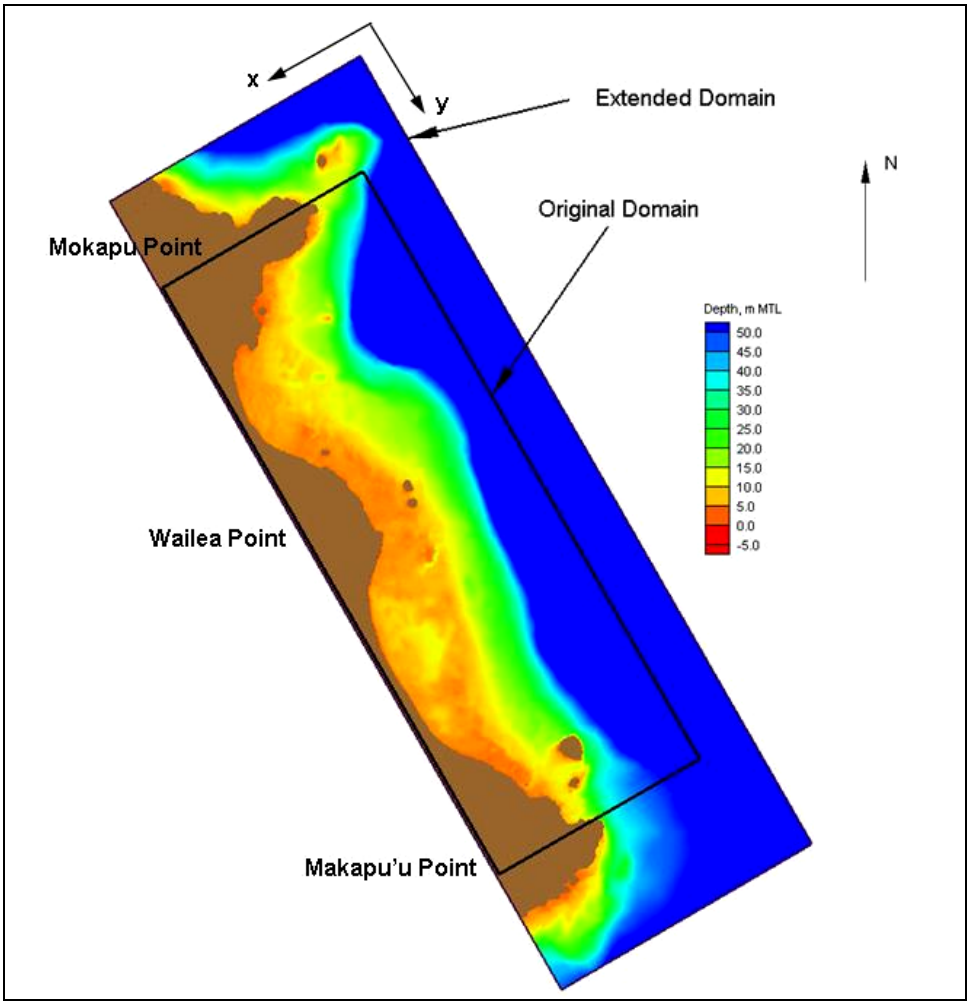

Figure 15. STWAVE grid domain.

For this study, the long-term data record (2000–2004) for Station 098 was analyzed with the Coastal Engineering and Data Analysis Software (CEDAS) 3.0 – Nearshore Evolution Modeling System (NEMOS) software. Since the purpose of this procedure was to determine all conditions that occurred at Station 098, the longest record possible, including the incomplete years 2000 and 2004, were included in the analysis. A 3-month gap in the data in 2004 and the small portion of 2005 data available at the time the study started (1 March 2005) were not included in the analysis.

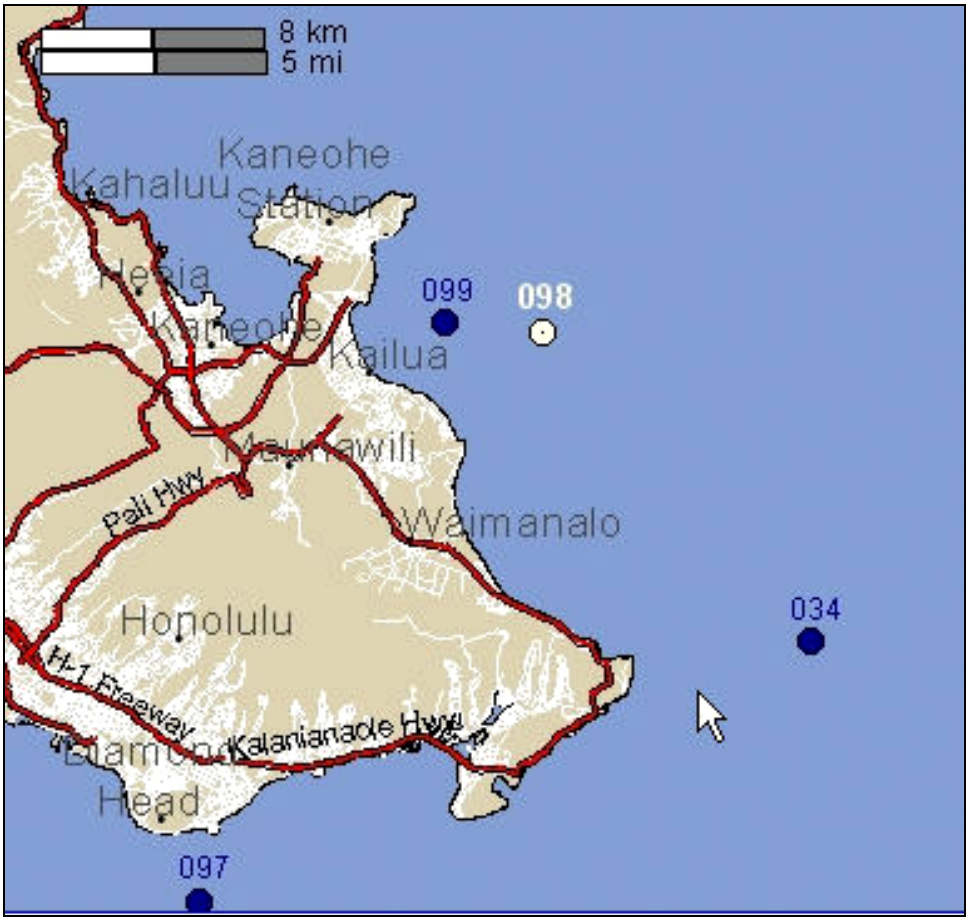

Figure 16. CDIP buoy locations courtesy of CDIP web site (http://cdip.ucsd.edu).

Figures 17 and 18 show that waves are generally from the east-northeast quadrant and range in height from 0.5 to 6.0 m. Peak wave periods are generally 6 to 16 sec. From these tabulations, a set of discrete conditions was selected for simulation (Table 2). From the 216 possible height-period-direction combinations, 134 conditions occurred in the 2000–2004 time period. The wave height range was defined at 0.5-m intervals from 0.75 m to 2.75 m and at a 0.75-m interval to 3.5 m. The wave period range was 6 to 16 sec at a 2-sec interval. The wave directions were incremented every 22.5 deg from -22.5 deg to 90 deg, relative to True North. For each of the 134 selected wave conditions, Texel Marsden Arsloe (TMA) shallow-water spectra were generated by applying the SMS spectral wave generation software, and with those spectra applied at the model boundary; wave transformation was simulated by applying STWAVE over the project domain.

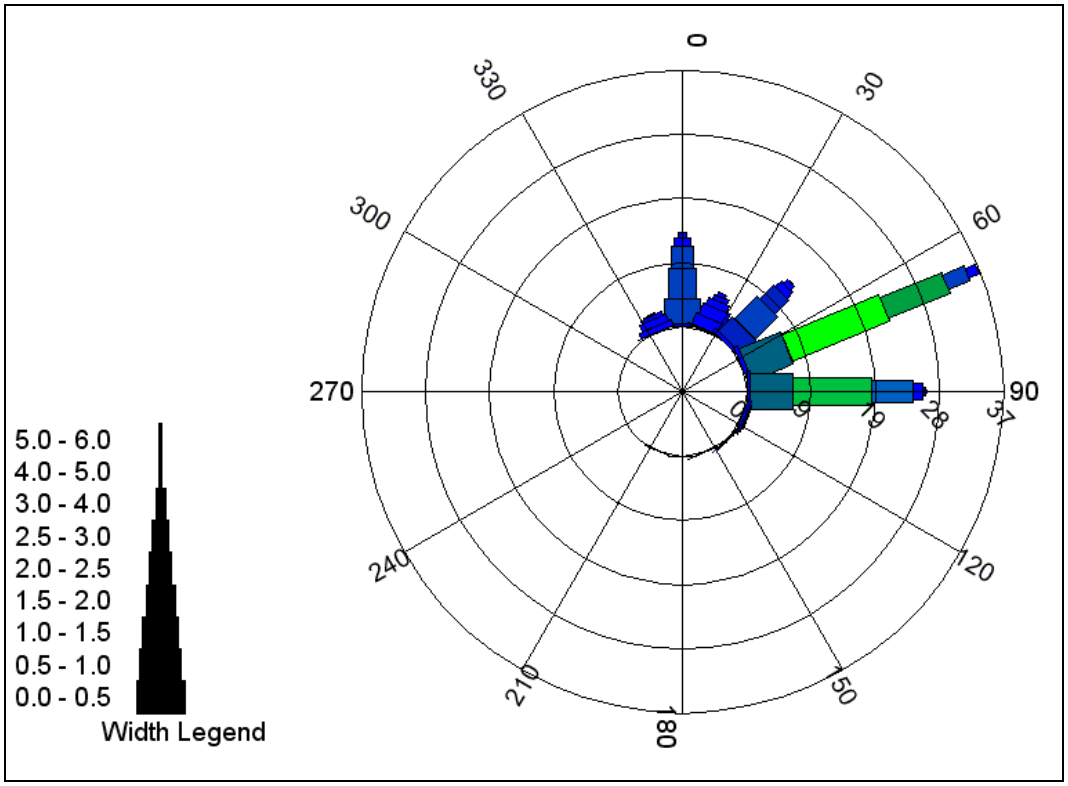

Figure 17. Wave height versus wave direction percent occurrence rose for CDIP Buoy 098 – Mokapu Point, HI (data from August 2000 through December 2004).

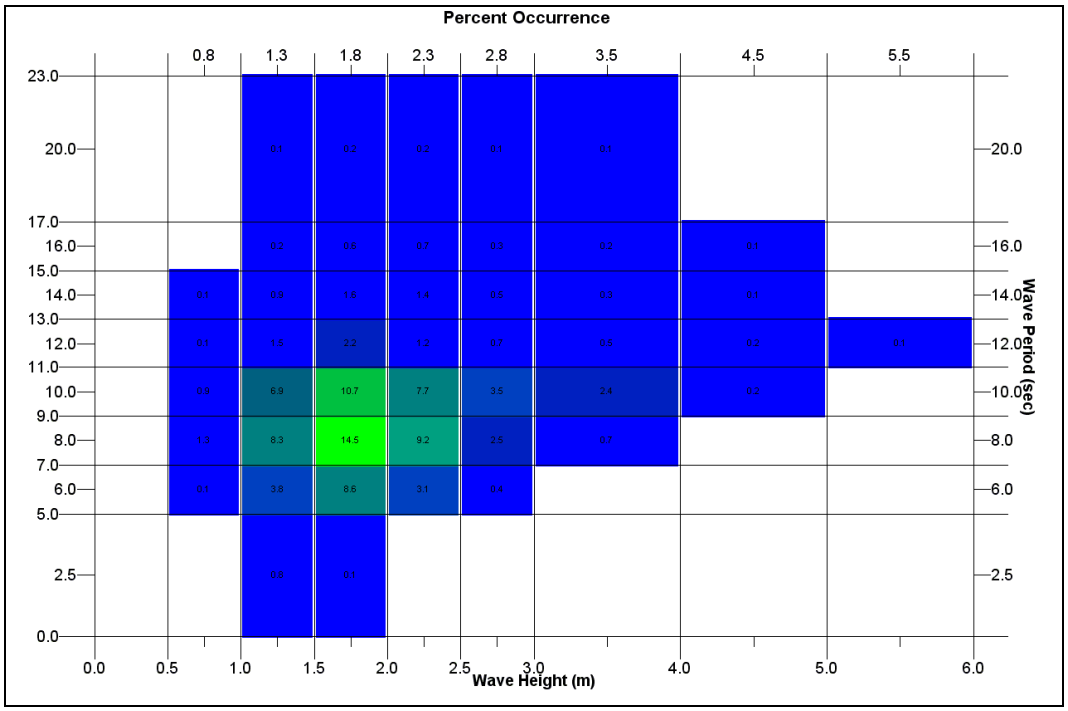

Figure 18. Block diagram of wave height versus wave period for CDIP Buoy 098 – Mokapu Point, HI (data from August 2000 through December 2004).

Table 2. Wave conditions.

Significant Wave Height, m	Wave Period sec	Wave Direction deg from North	Wave Direction deg from STWAVE axis
0.75	6	-22.5	82.5
1.25	8	0	60
1.75	10	22.5	37.5
2.25	12	45	15
2.75	14	67.5	-7.5
3.5	16	90	-30

Wave climate analysis

Nearshore conditions at a point in Waimanalo Bay [Figure 19, cell (229,506)] were extracted from the STWAVE model results for each of the 134 simulations. Since these simulations were to illustrate the technique for developing a wave climate, they did not include the detail of applying friction to the domain. A transformation correlation between the offshore

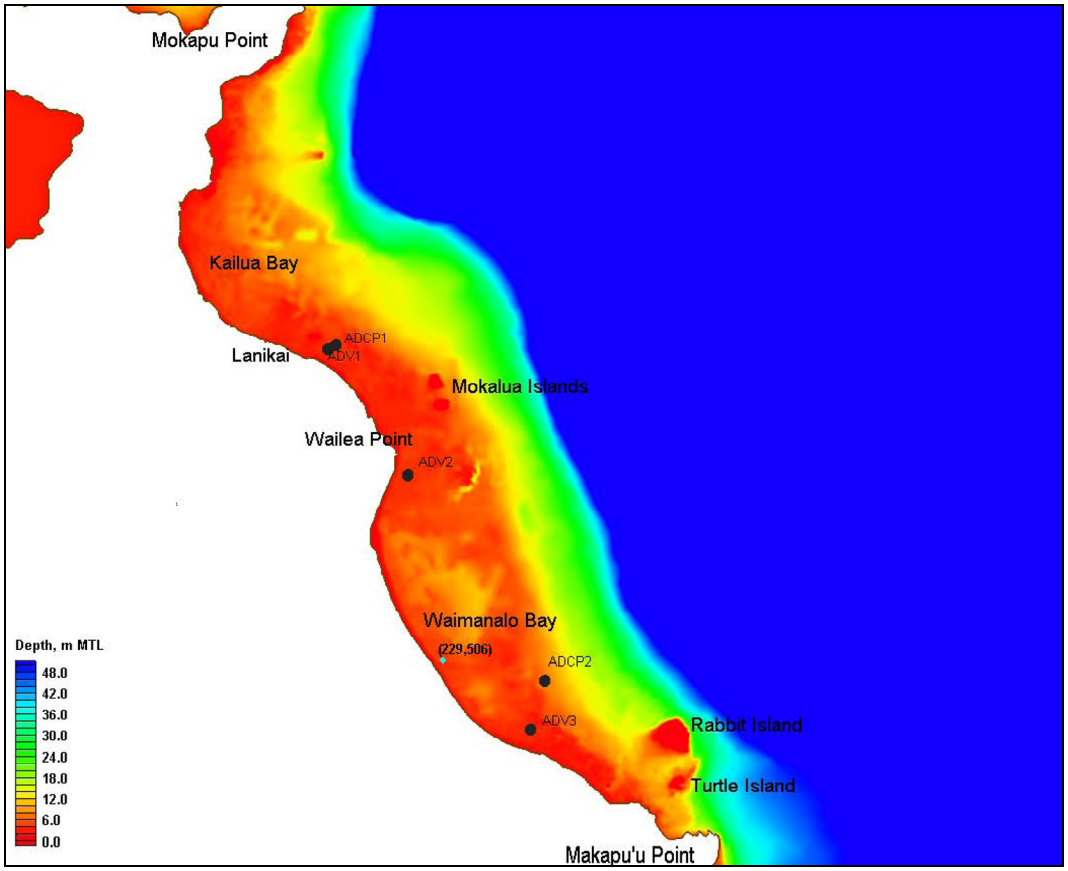

Figure 19. Location of extracted STWAVE model results (cell 229,506).

and nearshore conditions was then determined for each of the 134 simulations. By applying the appropriate transfer function to each wave condition in the 2000–2004 offshore time series at Station 098, a long-term (2000–2004) nearshore time series was generated (Figure 20). Note that the 3-month gap in the time series corresponds to 15 February to 19 May 2004 when the offshore CDIP Buoy 098 gauge was not operational. The nearshore time series demonstrates that there is a reduction in wave height from the offshore location to the nearshore location, landward of the extensive reef system due to depth-limited breaking and refraction. The time series, however, appears generally contained or banded between the 1.25 and 2.25 m wave height bins that were selected to represent the overall wave climate. Further analysis was required to determine if a more detailed representation of the offshore wave climate would better resolve the nearshore wave climate, and is discussed in the following.

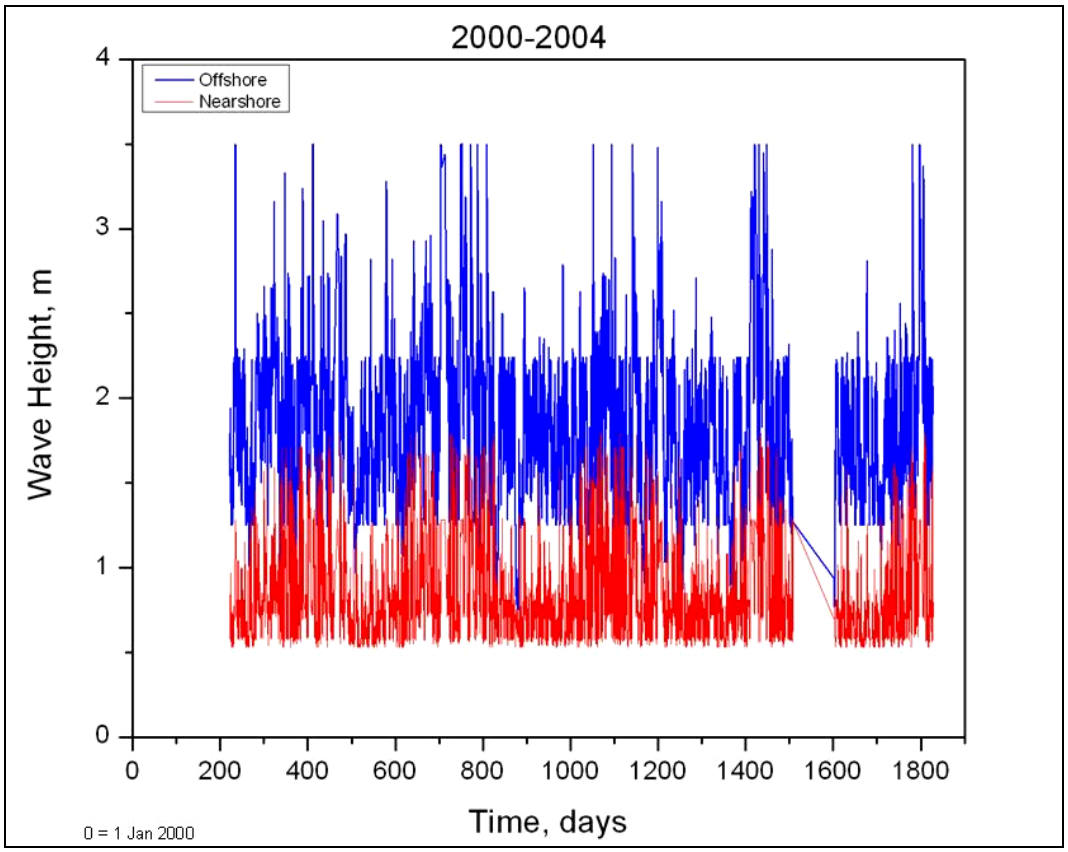

Figure 20. Nearshore time series (without friction) generated from offshore time series with 134 correlation conditions.

In order to capture the nearshore transformation time series more precisely and to include all wave conditions occurring in the time series, the range and refinement of the wave conditions simulated was expanded (Table 3). Wave heights ranged from 0.5 to 5.0 m with the finest increment being 0.25 m. Wave periods were expanded to include 20 sec. Wave angles were expanded to include waves from the east-southeasterly direction (representing waves 106–118 deg from True North) and were refined to 11.25 deg bands. For each of the 1274 selected wave conditions, TMA (shallow-water) spectra were generated by applying the SMS spectral wave generation software, and wave transformation was simulated by applying STWAVE over the project domain for each of the 1274 wave spectra. Again, nearshore conditions at cell (229,506) were extracted from the model results for each of the simulations. A transfer function between the offshore and nearshore conditions was then determined for each of the simulations. By applying the transfer function to each wave condition in the offshore time series at Station 098, a refined nearshore time series was generated (Figure 21), which shows a more realistic variation in the wave height. Note from the wave rose that wave directions converge to 35–73 deg relative to True North at the save point location shoreward of the reef and are predominantly directed shore-normal (60 deg). (In a follow-on study, the 1274 STWAVE simulations included bottom friction, and nearshore wave climates were developed for 10 nearshore locations.)

Table 3. Expanded (1274) wave conditions.

Significant Wave Height, m	Wave Period, sec	Wave Direction, deg from North	Wave Direction, deg from STWAVE axis
0.50	6	-22.5	82.5
0.75	8	-11.25	71.25
1.00	10	0	60
1.25	12	11.25	49.75
1.50	14	22.5	37.5
1.75	16	33.75	26.25
2.00	20	45	15
2.25		56.25	3.75
2.50		67.5	-7.5
2.75		78.75	-18.75
3.00		90	-30
3.50		101.25	-41.25
4.00		112.5	-52.5
5.00			

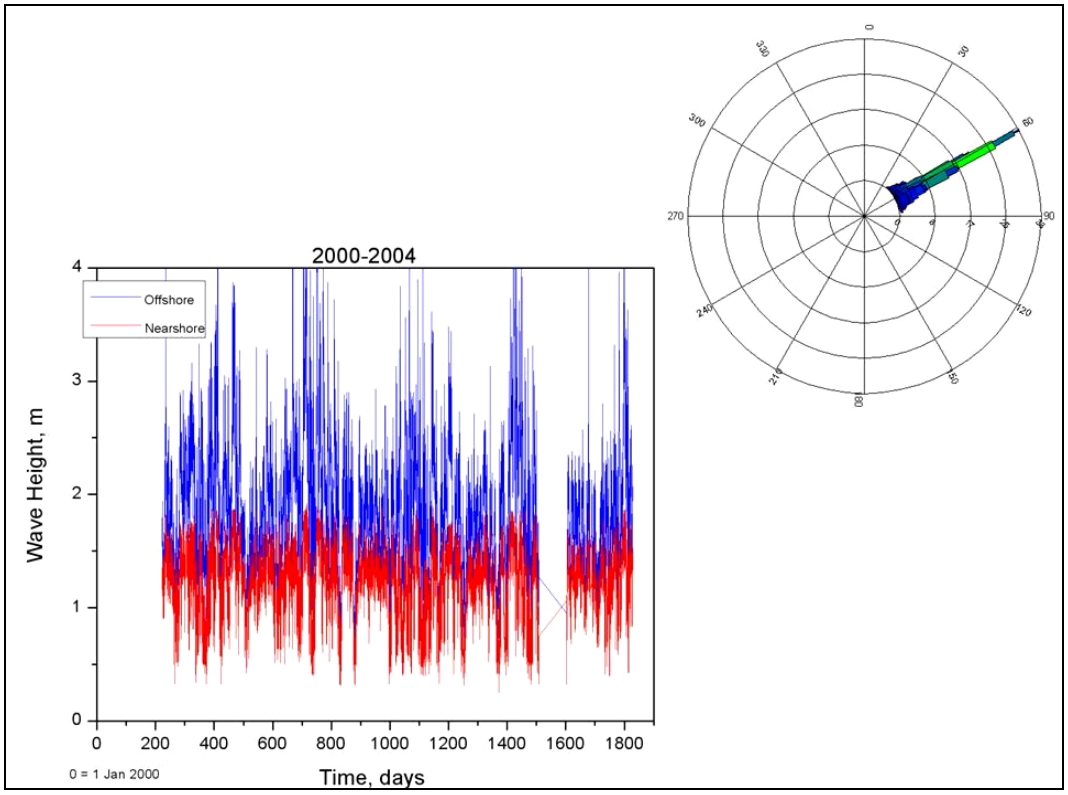

Figure 21. Nearshore time series (without friction) and wave rose generated from offshore time series with 1274 correlation conditions.

Bottom friction

Development of a bottom friction capability in STWAVE was completed for application to the extensive reefs in the SEO study area. STWAVE includes two formulations for bottom friction. The first is the JONSWAP formulation (Hasselmann et al. 1973; Padilla-Hernandez and Monbaliu 2001), where the spectral energy loss from bottom friction is formulated as a sink term, S_{bf}, in the energy balance equation,

$$S_{bf} = \frac{-1}{g} c_f \frac{\sigma^2}{\sinh^2 kd} E(f,\alpha) \tag{1}$$

where:

g = acceleration of gravity
c_f = bottom friction coefficient
σ = angular frequency
k = wave number
d = total water depth

E = spectral energy density divided by ($\rho_w\, g$), where ρ_w is density of water
f = wave frequency
α = wave direction.

The dissipation is summed over all frequencies and directions in the spectrum. A single friction coefficient, c_f, can be applied to the entire STWAVE domain, or a range of friction values can be applied on a cell-by-cell basis in a spatially varying manner. For the JONSWAP bottom friction formulation, c_f is specified as Γ/g, where the recommended values of Γ are in the range 0.038 to 0.067 m²/sec³ (or model input values of c_f = 0.004 to 0.007 m/sec) for sand beds based on the JONSWAP experiment and North Sea measurements (Hasselmann et al. 1973; Bouws and Komen 1983). Values of c_f applied for coral reefs range from 0.05 to 0.40 m/sec (Hardy 1993; Hearn 1999; Lowe et al. 2005). Equation 1 has a weak inverse dependence on water depth related to the increase in bottom wave orbital velocity as the relative depth, kd, decreases.

A Manning formulation is also available in STWAVE, based on Holthuijsen (2007),

$$S_{bf} = \frac{-1}{g}\left(\frac{gn^2}{d^{1/3}}\right)\frac{\sigma^2}{\sinh^2 kd}E(f,\alpha)u_{rms} \tag{2}$$

where the value of the Manning coefficient, n, is specified as input to STWAVE (either spatially constant or variable) and u_{rms} is the root-mean-square bottom velocity. With the Manning formulation, bottom friction dissipation has an additional inverse dependence on water depth. Estimates of Manning coefficients are available in most fluid mechanics reference books (e.g., 0.01 to 0.05 for smooth to rocky/weedy channels). Converting c_f values applied for coral reefs (0.05 to 0.40 m/sec) to Manning coefficients yields a range of 0.10 to 0.25. However, it is recommended that the specification of c_f or n be validated with field measurements. Application of this model capability to a specific site requires validation to field data.

A single friction value can be applied to the entire STWAVE domain or a range of friction values can be applied on a cell-by-cell basis. As an example, the 134 wave conditions first simulated were repeated with the revised STWAVE, applying a JONSWAP bottom friction coefficient typical for

reefs of c_f = 0.05 m/sec over the entire model domain. A comparison of nearshore waves at cell (229,506) was made (Figures 22 and 23). The offshore (blue) to nearshore without bottom friction (black) comparison shows a reduction in wave height of 38% (Figure 22). With bottom friction (red), the reduction in wave height is 84%. A comparison of the nearshore wave heights with and without bottom friction shows that, with the inclusion of bottom friction, wave heights range from 18–38% of the previous results that did not include bottom friction. On average, the wave height was 26% of the frictionless value at the selected location. Waves refract less with the inclusion of bottom friction, likely due to the reduction in energy at lower frequency (Figure 23).

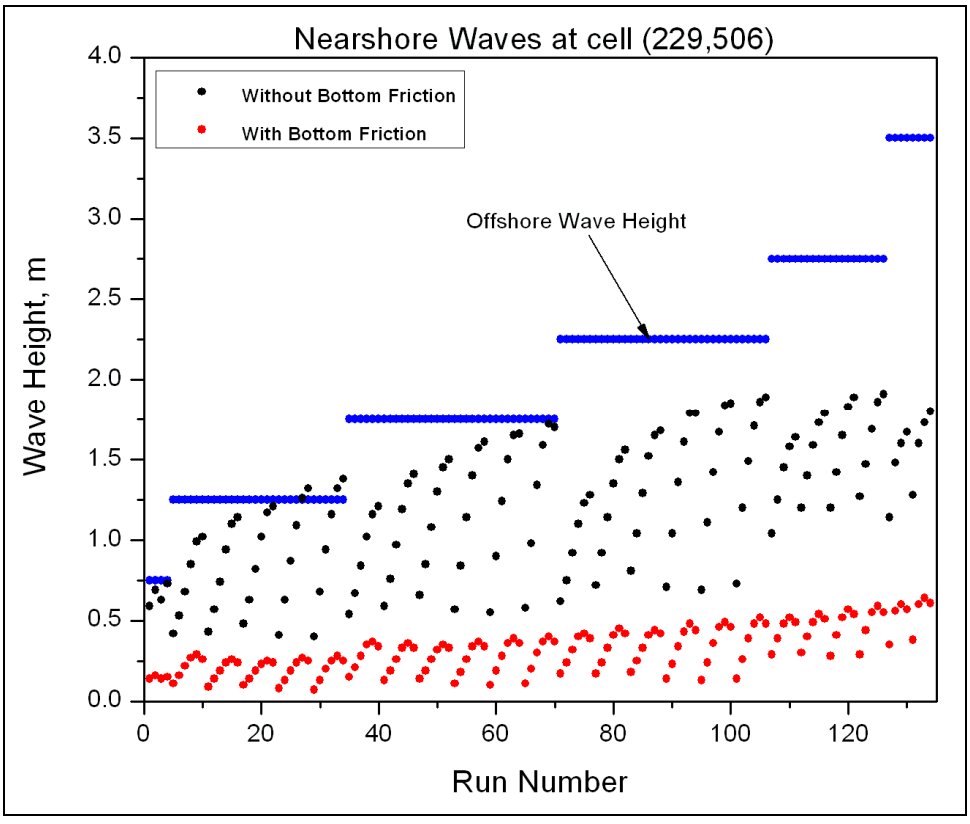

Figure 22. Comparison of predicted wave heights at cell (229,506) with and without the STWAVE bottom friction feature.

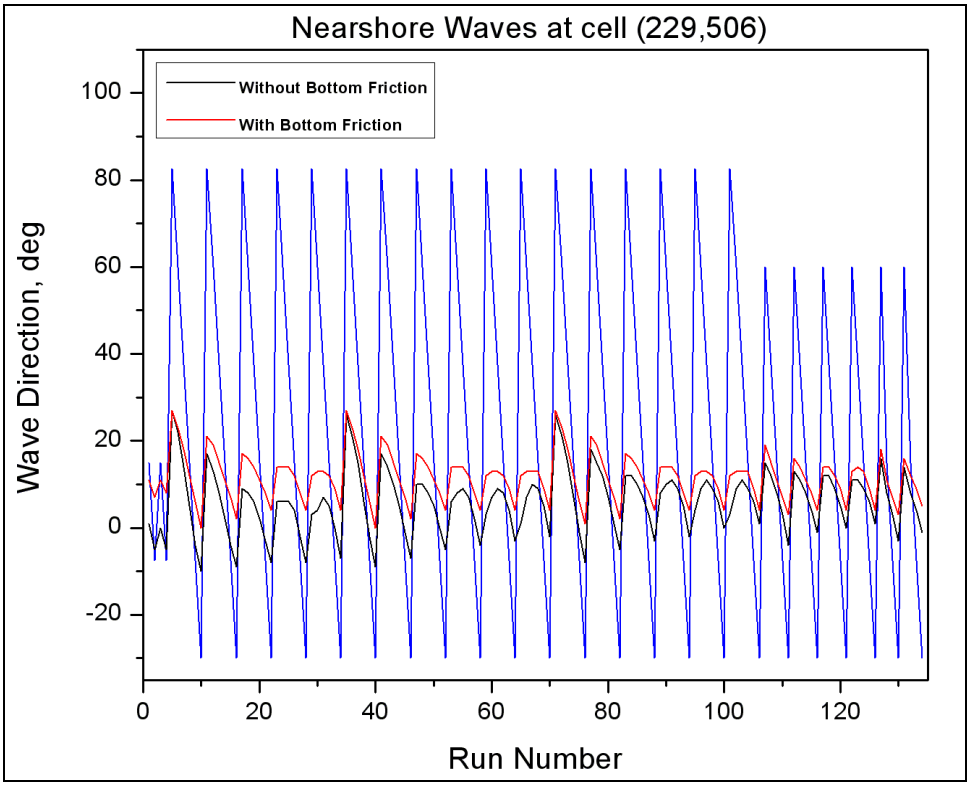

Figure 23. Comparison of predicted wave direction at cell (229,506) with and without the STWAVE bottom friction feature.

As another example, for each of the 1274 selected wave conditions simulated subsequently to achieve a more detailed wave climate, wave transformation *including spatially constant bottom friction* of 0.05 m/sec was simulated by applying STWAVE over the project domain for each of the 1274 wave spectra. Again, nearshore conditions at cell (229,506) were extracted from the model results for each of the simulations. A transfer function between the offshore and nearshore condition was then determined for each of the simulations. By applying the transfer function to each wave condition in the offshore time series at Station 098, a refined nearshore time series with bottom friction was generated (Figure 24). A comparison of Figures 21 and 24 shows that the constant 0.05 value for the JONSWAP bottom friction coefficient reduces nearshore wave heights by approximately 73%.

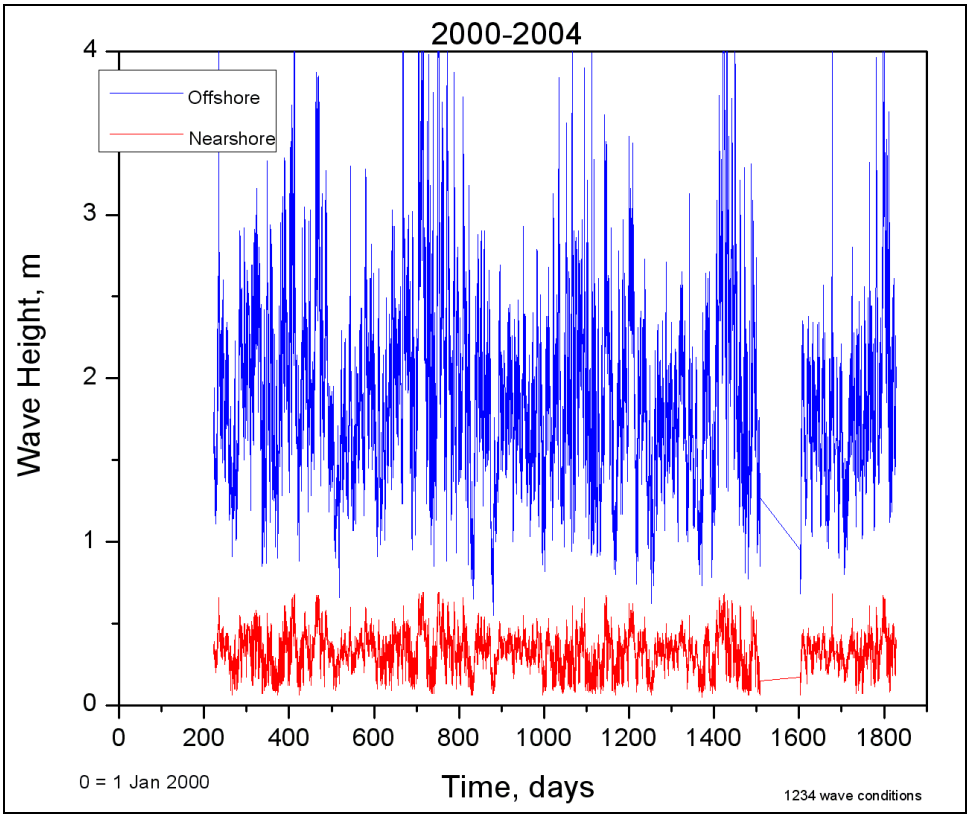

Figure 24. Nearshore time series (including spatially constant bottom friction) generated from offshore time series with 1274 correlation conditions.

Model validation

As previously discussed, the extended domain STWAVE grid was applied in the model validation process. The August 2005 model validation time period corresponded to a portion of the field data collection time period (9 August through 14 September 2005). CDIP Buoy data for August 2005 (Figure 25) were extracted from the CDIP website for every 3-hr interval of August 2005. For each of these measured wave conditions, TMA (shallow-water) spectra were generated by applying the SMS spectral wave generation software. These spectra were then applied to the offshore boundary of the model domain. Note that analysis was done to compare the waves at the 300-m depth STWAVE boundary and the 100-m depth gauge location by applying the University of Delaware Hydrodynamic Wave Calculator applet application (http://www.coastal.udel.edu/faculty/rad/wavetheory.html). It was found that the difference in wave height from the 300-m to 100-m depth is small (approximately 4% for periods <15 sec, which accounts for 98% of the waves) and the offshore gauge data were applied at the STWAVE boundary without back refracting to the 300-m water depth.

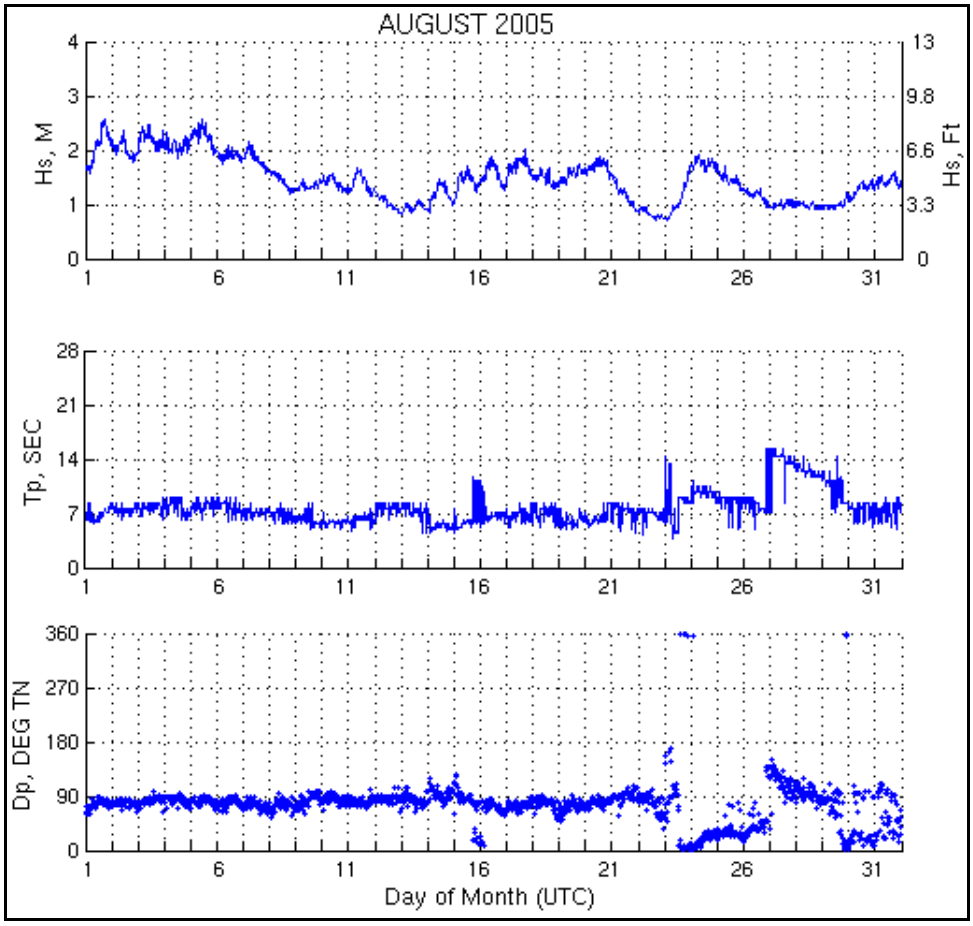

Figure 25. CDIP buoy data at station 098 (Mokapu Point, Hawaii) for August 2005.

Initially, a constant bottom friction value was applied to each cell of the STWAVE domain. Several simulations with different constant JONSWAP bottom friction values ranging from 0.04 to 0.12 m/sec were made to examine the range of response (wave height) at the gauge locations. Figure 26 shows the wave height time series generated by STWAVE at the location where ADV1 was placed, without bottom friction and for four simulations with bottom friction. These initial simulations indicated that, without bottom friction, wave heights at ADV1 are reduced on average by 21% relative to the offshore wave height due to depth-limited breaking. Bottom friction reduces wave height at ADV1's location by 64% for a JONSWAP bottom friction coefficient of 0.04 m/sec (wave height is 36% of the offshore wave height), by 71–76% for a bottom friction value of 0.05 m/sec (wave height is 24–29% of the offshore wave height), and by 93% for a bottom friction value of 0.12 m/sec (wave height is 7% of the offshore wave height). Applying a Manning friction coefficient of 0.15 to 0.25 to the reef resulted in average wave height reductions of 62–80%.

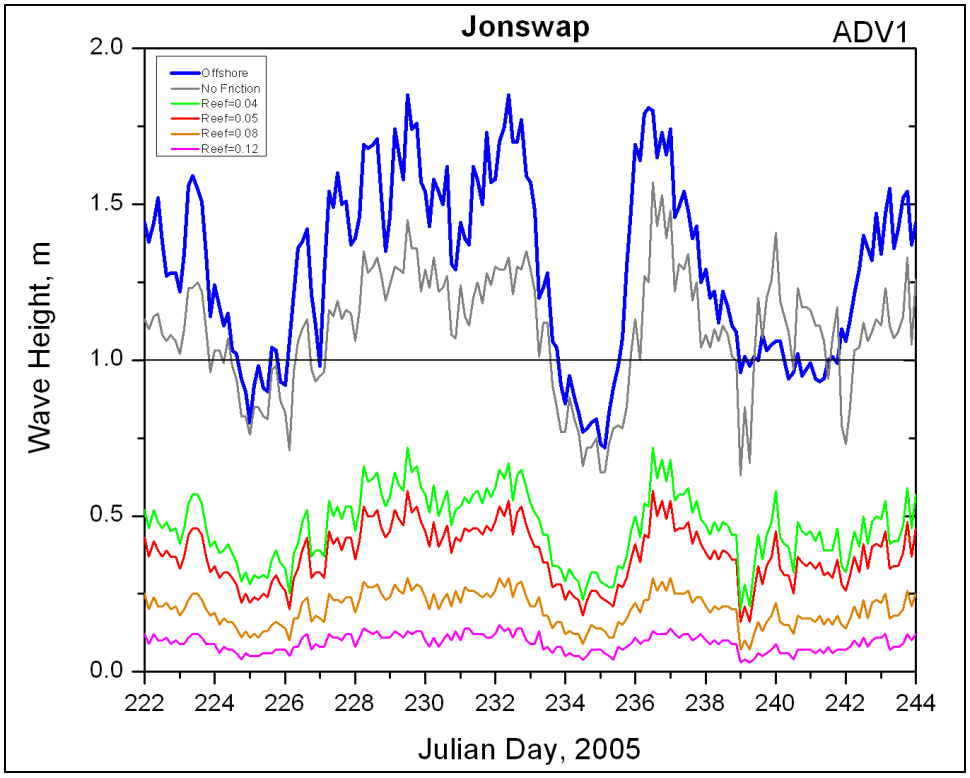

Figure 26. Simulated wave height time series at ADV1 with and without bottom friction.

The range of response indicates the importance of selecting the appropriate bottom friction value to represent the reefs in the study area. In addition, a variable friction field with a larger friction value applied only over the reef areas would be the most appropriate representation of the study area.

In the first set of validation simulations, a variable bottom friction field with JONSWAP friction coefficients of 0.05 m/sec applied to the reef region, 0.09 m/sec around the offshore islands (for compatibility/linkage to the ADCIRC model), and 0.006 m/sec in the offshore regions was utilized. A Manning validation simulation was also made with friction coefficients of 0.20 applied to the reef region (which is within the valid range of reef coefficients applied in the literature), 0.19 around the offshore islands, and 0.02 in the offshore regions. The simulations also included water level fluctuation due to tide. A comparison of field data collected at the three ADV locations (Figure 19) to the simulated wave heights was made. Figures 27–32 show the wave height time series generated by STWAVE at the gauge locations without bottom friction and for two simulations with bottom friction (with and without tide), along with the field measurements at these locations.

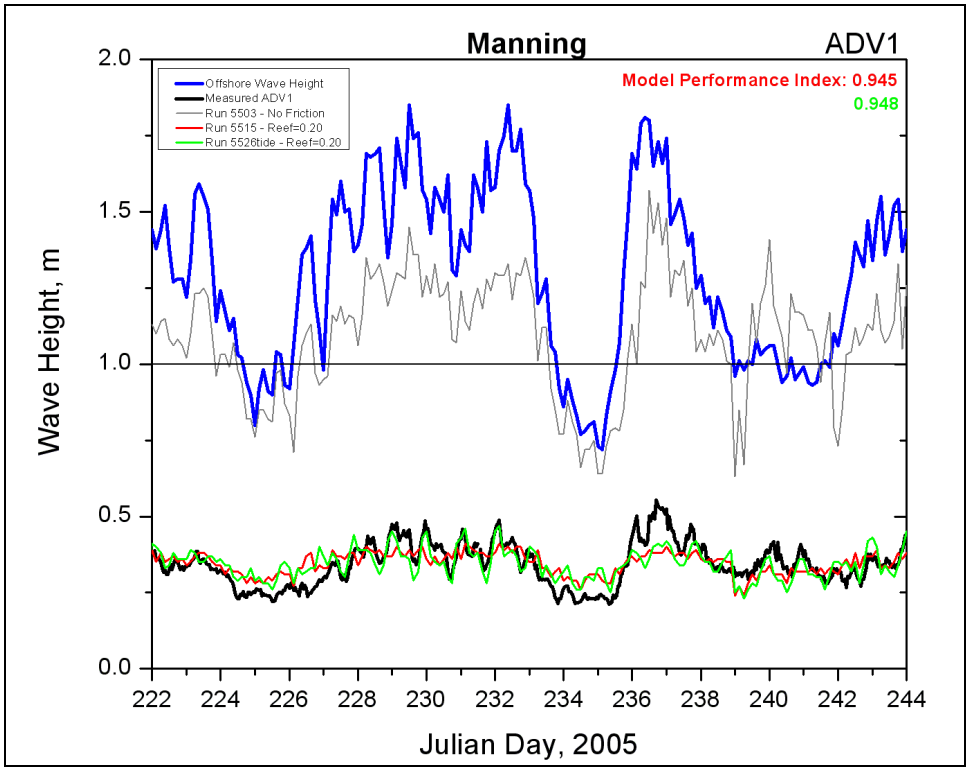

Figure 27. Comparison of measurements and STWAVE results at ADV1 with reef Manning bottom friction coefficient of 0.20.

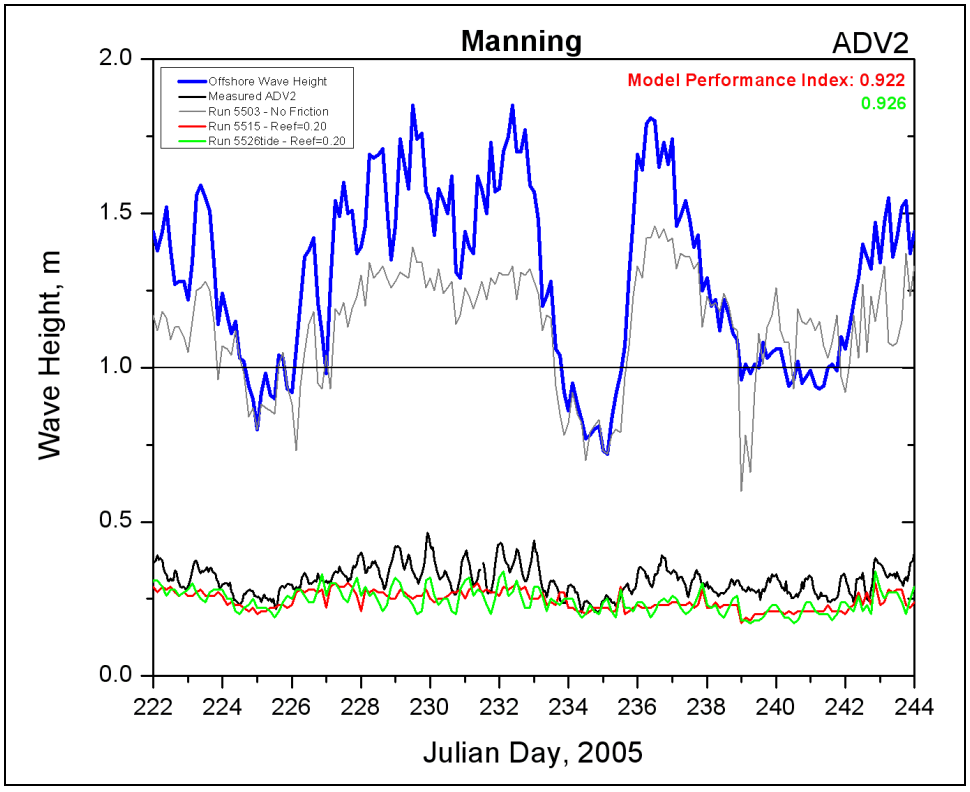

Figure 28. Comparison of measurements and STWAVE results at ADV2 with reef Manning bottom friction coefficient of 0.20.

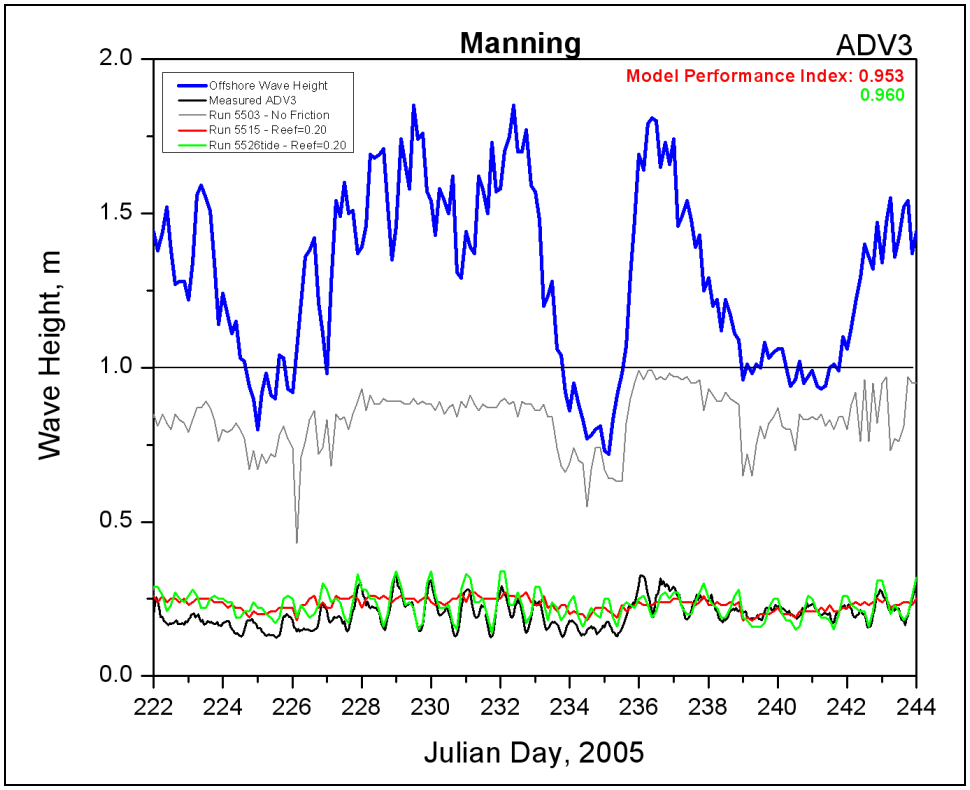

Figure 29. Comparison of measurements and STWAVE results at ADV3 with reef Manning bottom friction coefficient of 0.20.

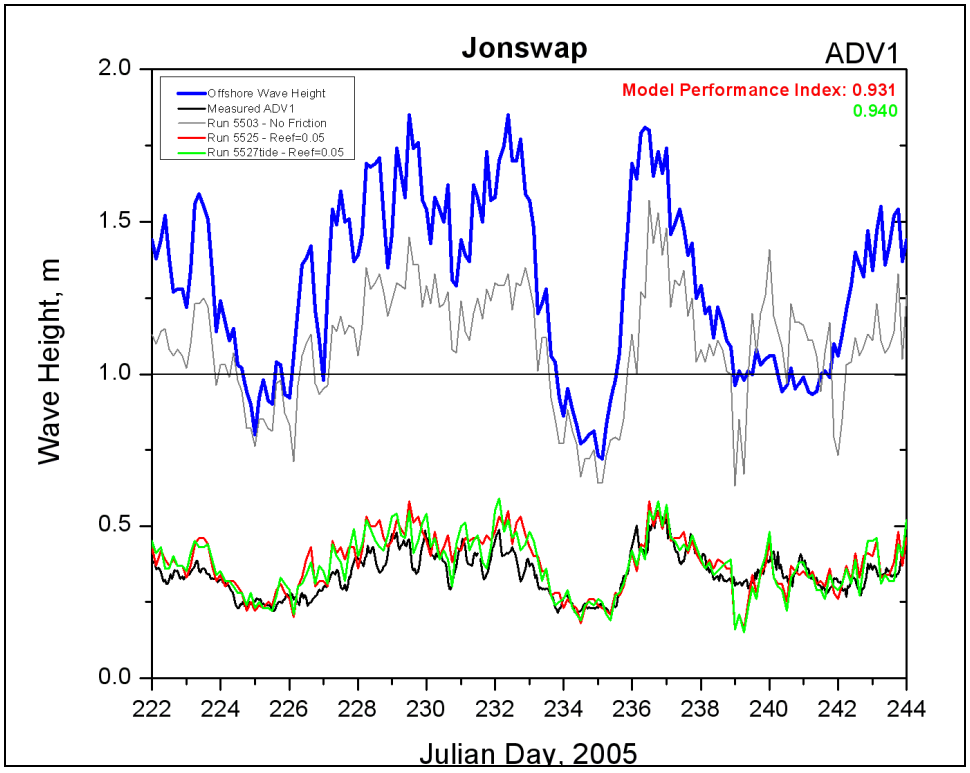

Figure 30. Comparison of measurements and STWAVE results at ADV1 f with reef JONSWAP bottom friction coefficient of 0.05.

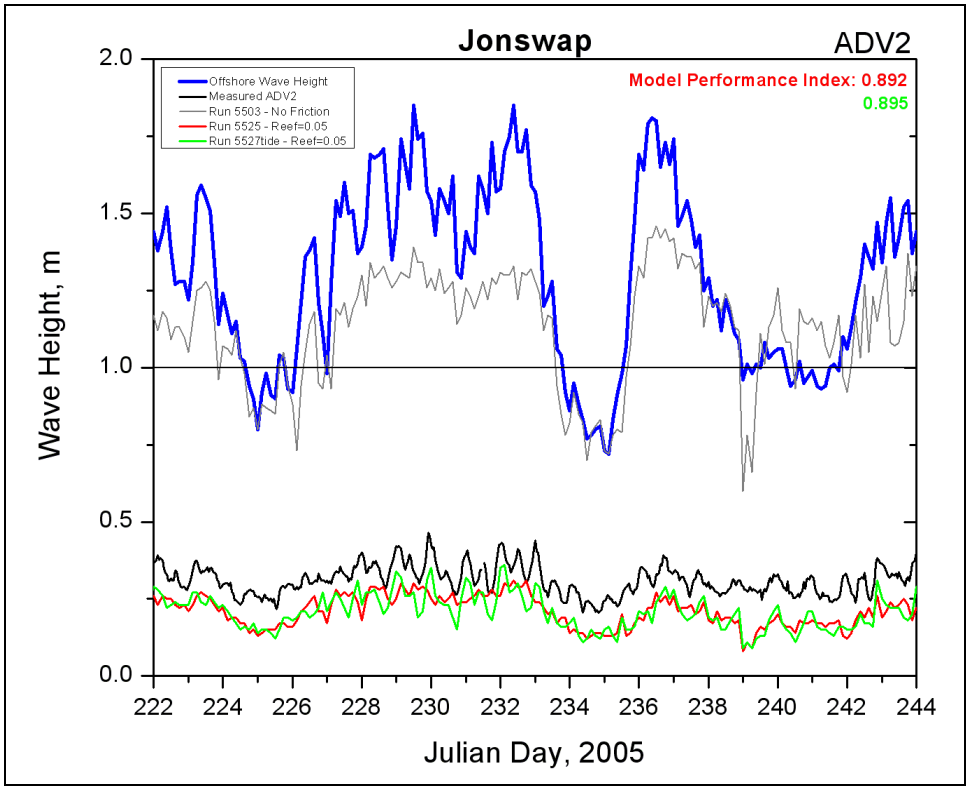

Figure 31. Comparison of measurements and STWAVE results at ADV2 with reef JONSWAP bottom friction coefficient of 0.05.

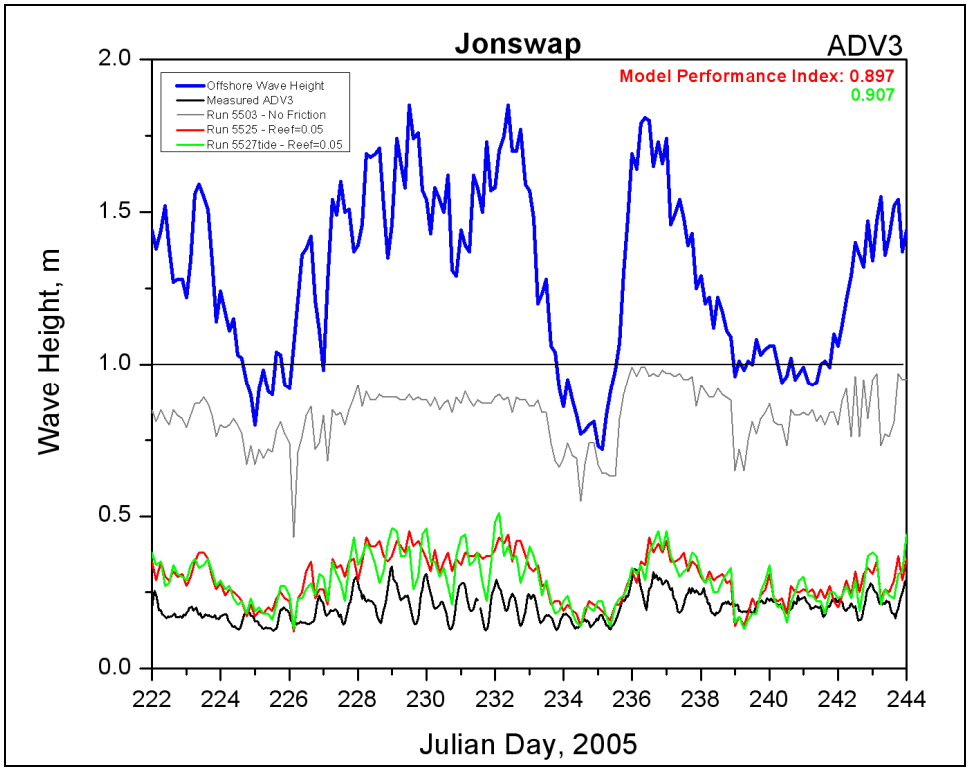

Figure 32. Comparison of measurements and STWAVE results at ADV3 with reef JONSWAP bottom friction coefficient of 0.05.

The field measurements range in wave height from 0.12 to 0.69 m for the data collection time period and the model results range from 0.08 to 0.59 m. The STWAVE model captures the large reduction in wave height from the offshore location to the three nearshore locations. The model results for the ADV1 location follow the magnitude and trend of the data well, particularly with the JONSWAP friction formulation. The inclusion of tidal fluctuation in the model improves the comparison to gauge data, particularly with the Manning friction formulation. Model results at the ADV2 location tend to underpredict the measured wave height with the selected validation friction coefficient. Model results at the ADV2 location show greater wave height variation with time, whereas the measurements show much less variability. Model results at ADV3 tend to over-predict the measured wave height when the offshore waves are greater than 1.3 m.

Another indicator of the model ability to estimate wave transformation over a reef is the Model Performance Index (MPI) (Smith 2000). The MPI is a measure of the models ability to capture the transformation from offshore to nearshore that is observed in the field data.

$$\text{MPI} = (1 - Error_{rms})/Changes_{rms} \quad (3)$$

where $Error_{rms}$ is the root-mean-square error of the model compared to the ADV gauge data and $Changes_{rms}$ is the root-mean-square change from the offshore data to the nearshore data. Values of the MPI near unity indicate good agreement. For the initial simulations with constant bottom friction applied to the reef, the MPI values are 0.92 to 0.96 for the Manning representation of bottom friction (n = 0.20) and 0.89 to 0.94 for the JONSWAP representation of bottom friction (c_f = 0.05).

Improvements to the results, particularly at ADV3, could be made by revising the friction coefficients to represent the spatial variability of the reef roughness. (The coral reefs in this region are described as “mushroom fields.” Some areas of the reef are more solid and some areas have gaps and holes in the reef.) Without detailed knowledge of the contiguous/noncontiguous areas of the reef, an educated attempt was made to represent the variations in the reef. The center section of the reef was given a smaller friction coefficient and the southern portion of the reef was given a larger coefficient (Figure 33). These adjusted values were selected based upon the under/overprediction of wave height at ADV2 and ADV3,

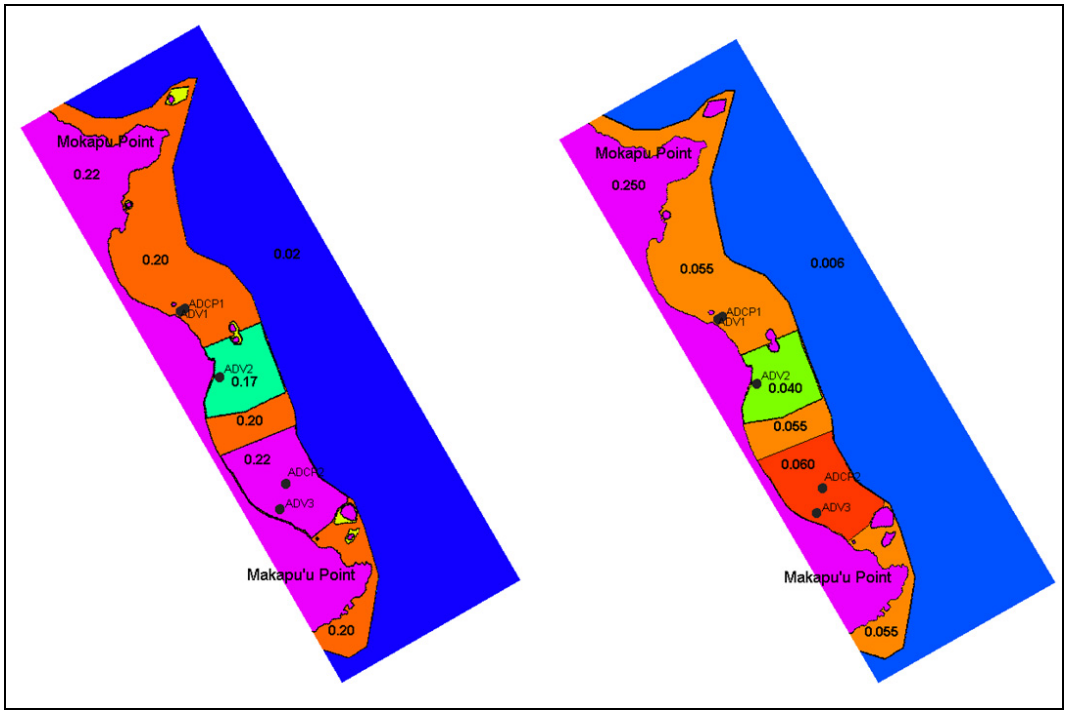

Figure 33. Variable Manning (left) and JONSWAP (right) friction fields.

respectively, in the previous simulation. The final validation simulation was made with JONSWAP friction coefficients of 0.04/0.055/0.06 variably applied to the reef region, 0.09 around the offshore islands (for compatibility/linkage to the ADCIRC model), and 0.006 in the offshore regions. A Manning validation simulation was also made with variable friction coefficients of 0.17/0.20/0.22 applied to the reef region, 0.19 around the offshore islands, and 0.02 in the offshore regions. Tidal fluctuation was included in these simulations.

As shown in Figures 34–39, with a variable bottom friction coefficient to represent variability in the reef structure, model results compare extremely well with the data at all three gauge locations with both the Manning and the JONSWAP friction formulations. The MPI values are 0.948 to 0.970 for the Manning simulations and 0.951 to 0.953 for the JONSWAP simulations. The magnitude and trend as well as the tidal fluctuation exhibited by the data are all captured by the model.

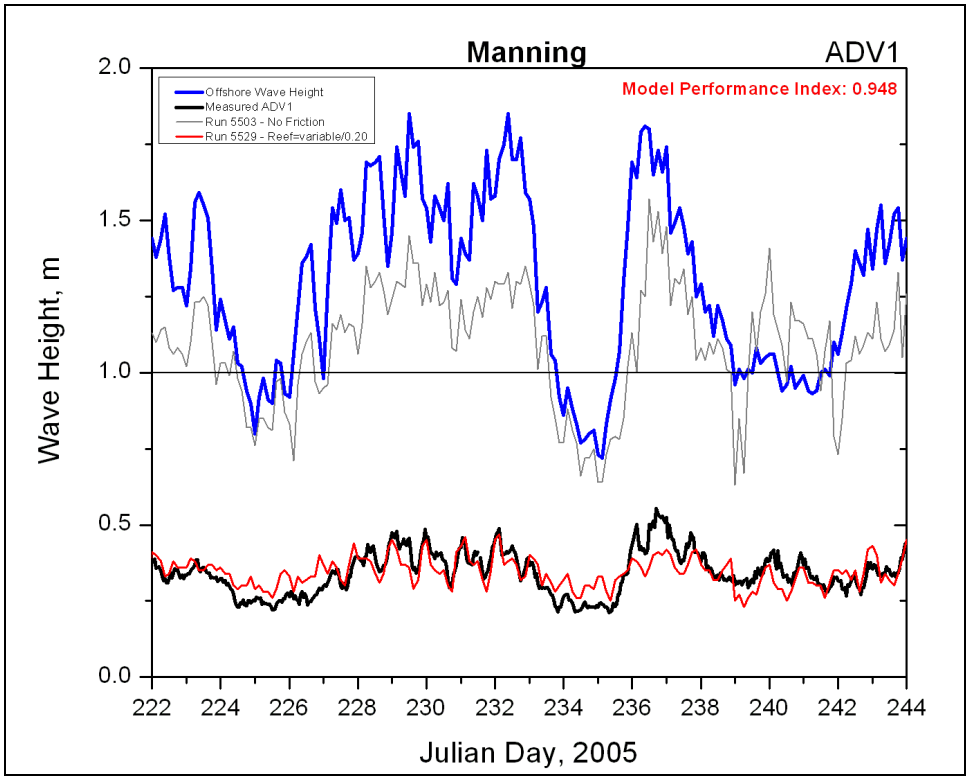

Figure 34. Comparison of measurements and STWAVE results at ADV1 for spatially varying Manning bottom friction.

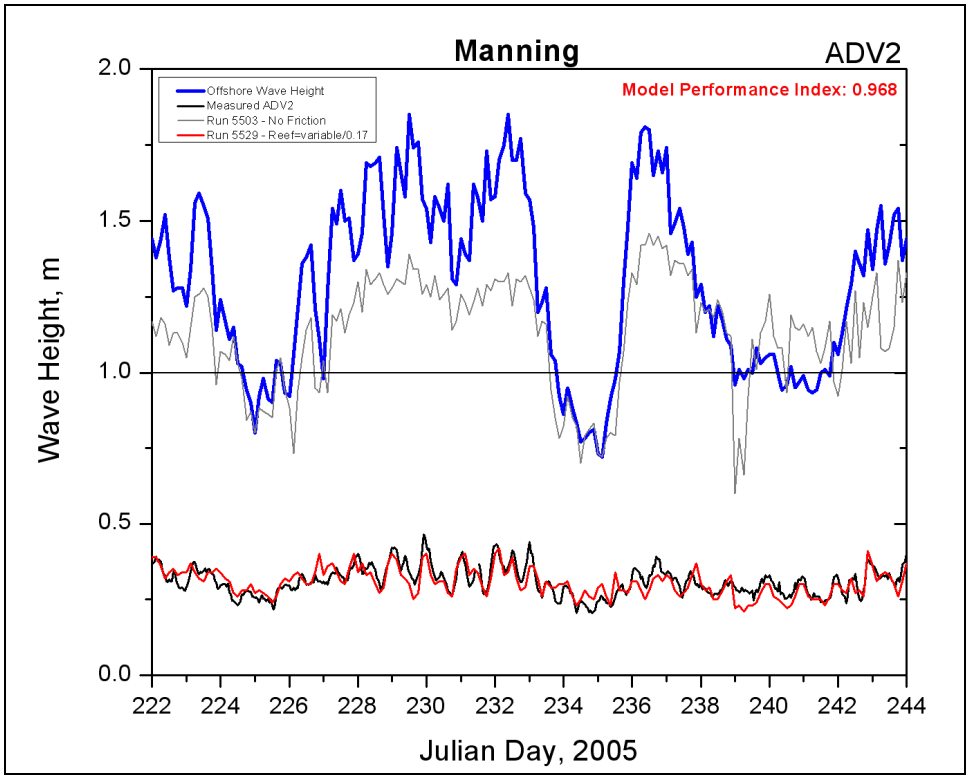

Figure 35. Comparison of measurements and STWAVE results at ADV2 for spatially varying Manning bottom friction.

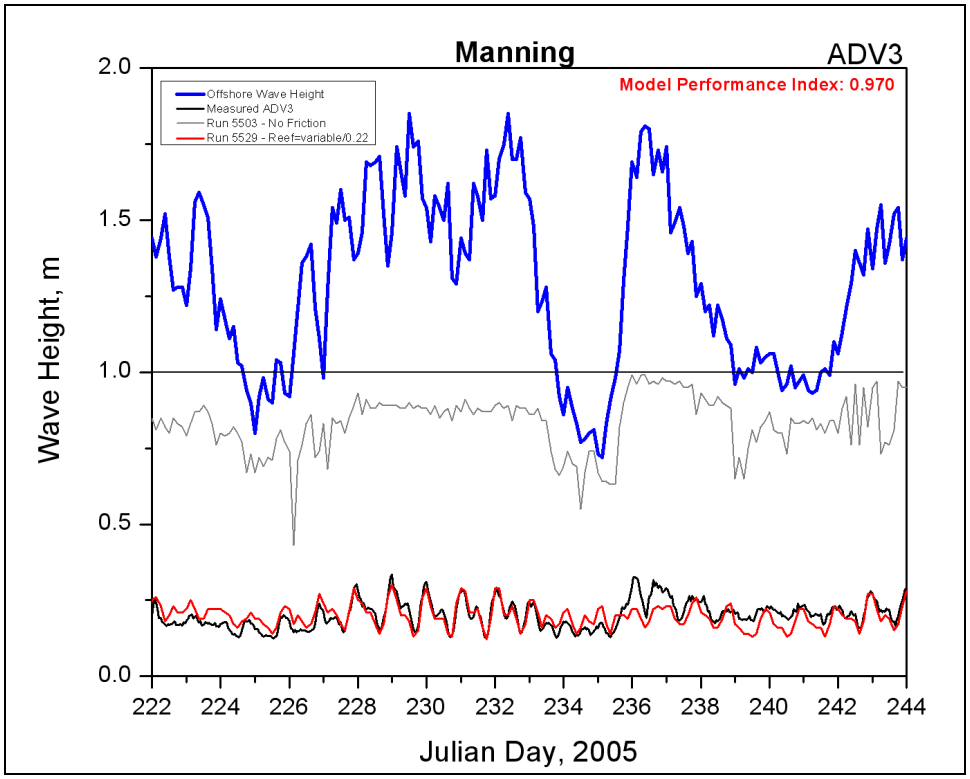

Figure 36. Comparison of measurements and STWAVE results at ADV3 for spatially varying Manning bottom friction.

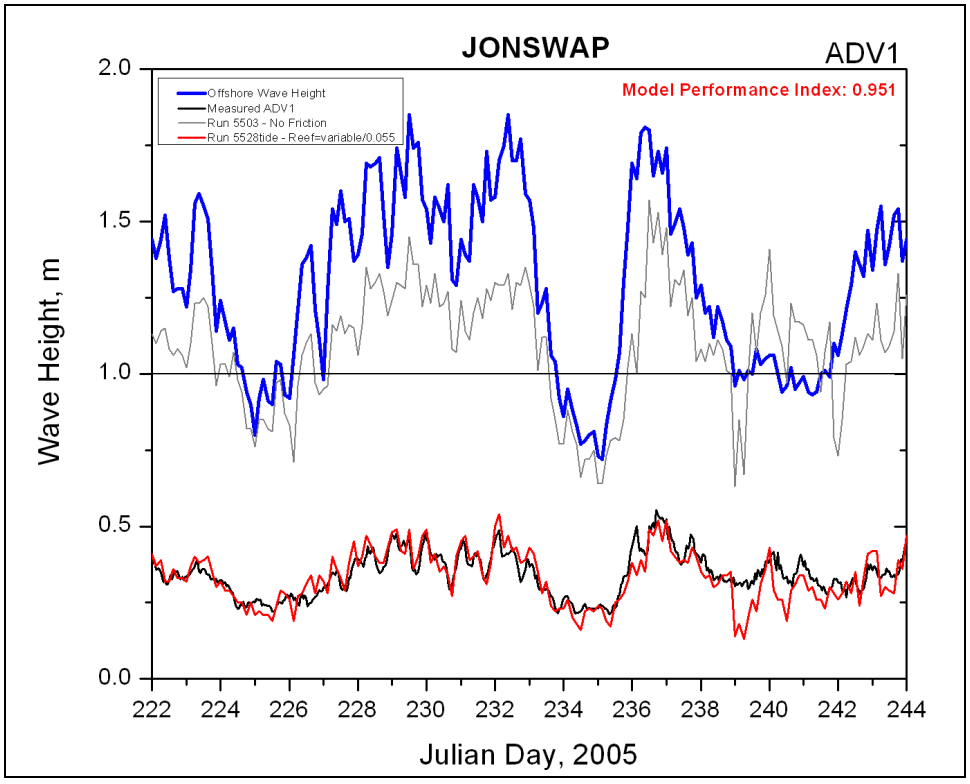

Figure 37. Comparison of measurements and STWAVE results at ADV1 for spatially varying JONSWAP bottom friction.

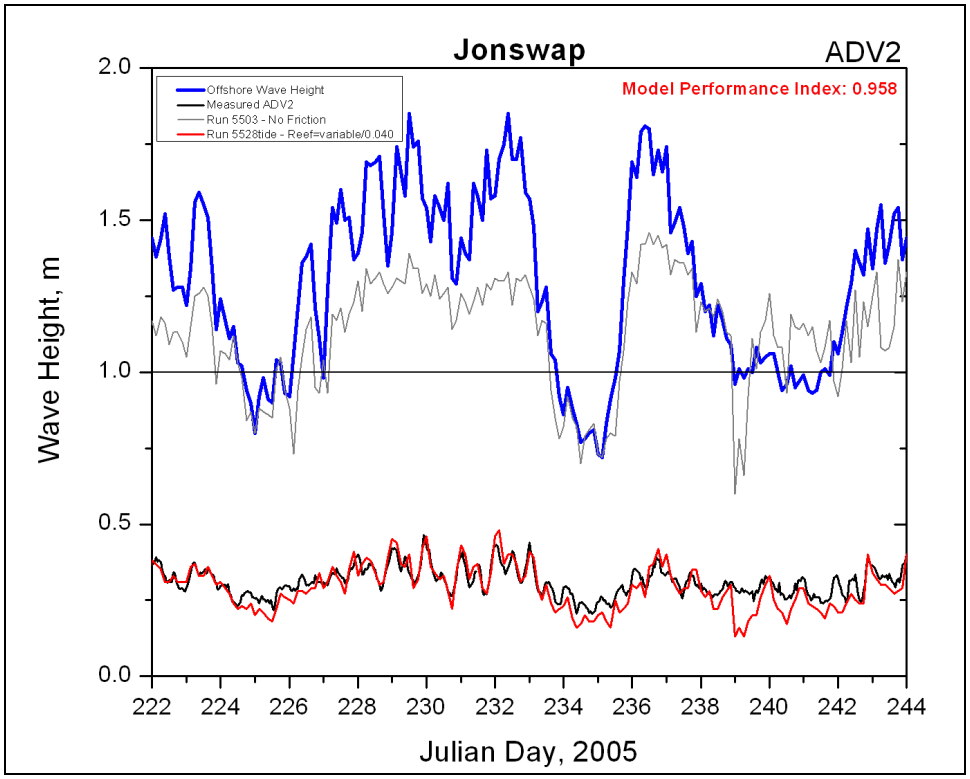

Figure 38. Comparison of measurements and STWAVE results at ADV2 for spatially varying JONSWAP bottom friction.

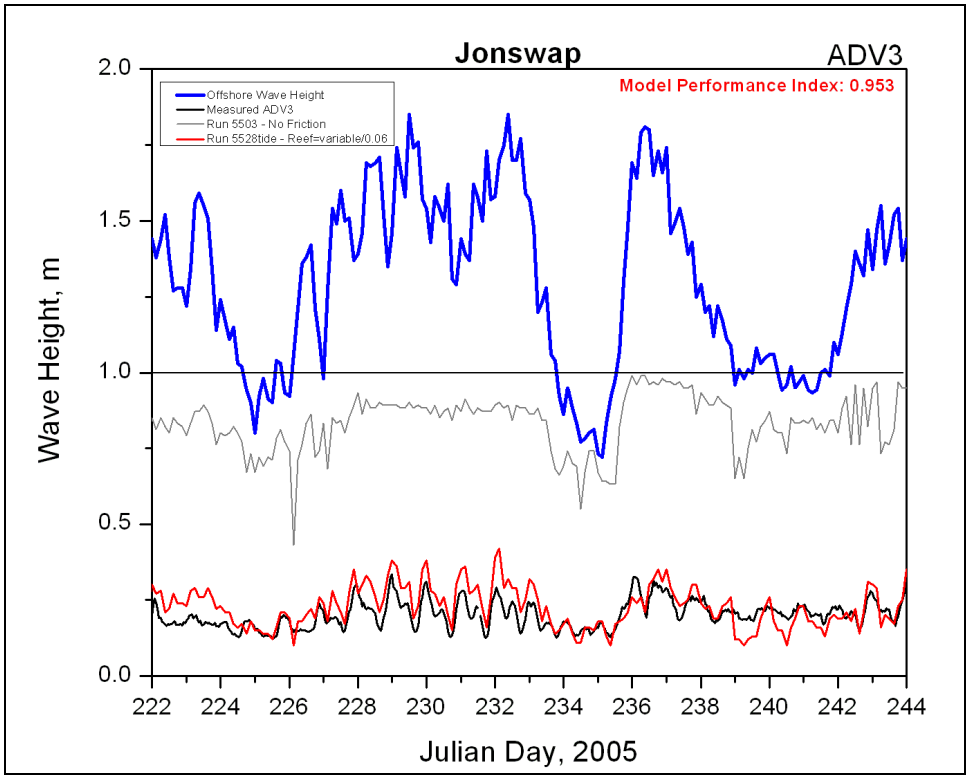

Figure 39. Comparison of measurements and STWAVE results at ADV3 for spatially varying JONSWAP bottom friction.

ADCIRC validation – wind, tide, and waves for gauge deployment time period

In the final validation, ADCIRC was applied to the study area for the August 2005 time period. This month overlapped the gauge deployment time period by approximately 2.5 weeks. ADCIRC was forced along the open boundary with tidal variation data extracted from the LeProvost tidal database. Wind speed and direction information were obtained from the OWI winds described in the wind sources section earlier in this document. Wave forcing information was provided from the STWAVE simulation driven by CDIP Buoy 098 data. A series of ADCIRC simulations were run for the selected month in the validation procedure. The ADCIRC simulations varied in the hydrodynamic parameters, bottom friction values, including with and without wind and wave forcing as part of this validation process. Some issues with the steep bathymetric gradients near the offshore island caused energetic wave breaking and created large radiation stress gradients, which led to ADCIRC model instability. This was overcome by applying a large bottom friction value (0.09) in STWAVE near the offshore islands and limiting radiation stress gradients to a maximum of 0.0001 m^2/sec^2. The final ADCIRC simulation applied a hybrid bottom friction formulation with a minimum c_f value of 0.003 m/sec (similar to the minimum value applied in the STWAVE validation — 0.006 m/sec), then increased in value in shallow depths (less than 1.0 m). The eddy viscosity was set to 4.0 m^2/sec, and the time step was 0.4 sec.

Simulation analysis

Currents and water levels were compared with field data obtained from the gauge deployment described earlier. Calculated water levels compared well in range and phase to measurements, but underestimated some lower peaks while overestimating some higher peaks. This may have been caused by localized interaction of the tides with the reefs surrounding the gauge locations. Water level comparisons with the three ADV gauges are shown in Figures 40–42. A harmonic analysis may prove useful in obtaining a better comparison to the tidal constituents. However, since the measured current velocities are so small, an improved tidal constituent forcing would not greatly influence the total range of water level and therefore would not increase the current velocities significantly. Therefore, no harmonic analysis was performed.

Current velocity data from the three ADV gauges (near-bottom point measurements) and two ADCP gauges (depth-averaged) were extremely small during the overlapping deployment time period—generally less than 10 cm/sec. (The near-bottom ADV measurements would be expected to be lower than depth-averaged values and therefore less than the ADCIRC-computed values.) Due to these small measured depth-averaged current magnitudes, depth-averaged current velocities calculated at these locations from the ADCIRC circulation model were not expected to compare well; however, the range of velocity model results (0.2–27.2 cm/sec) is well within one order of magnitude of the range of measurements (0.1–16.8 cm/sec) and generally very close to the measurements. Comparisons of ADCIRC circulation results to ADV and ADCP gauge measurements are shown in Figures 43–47. Note that this analysis indicates that tidal and wave-induced currents for this time period were not significant enough in this region to bring forward to sediment transport analysis. This reaffirms the typical conclusion that potential sediment transport mechanisms are more likely to be waves and storm-induced currents for the open coast. A follow-on study to examine the effects of waves and storm-induced currents on sediment transport is ongoing.

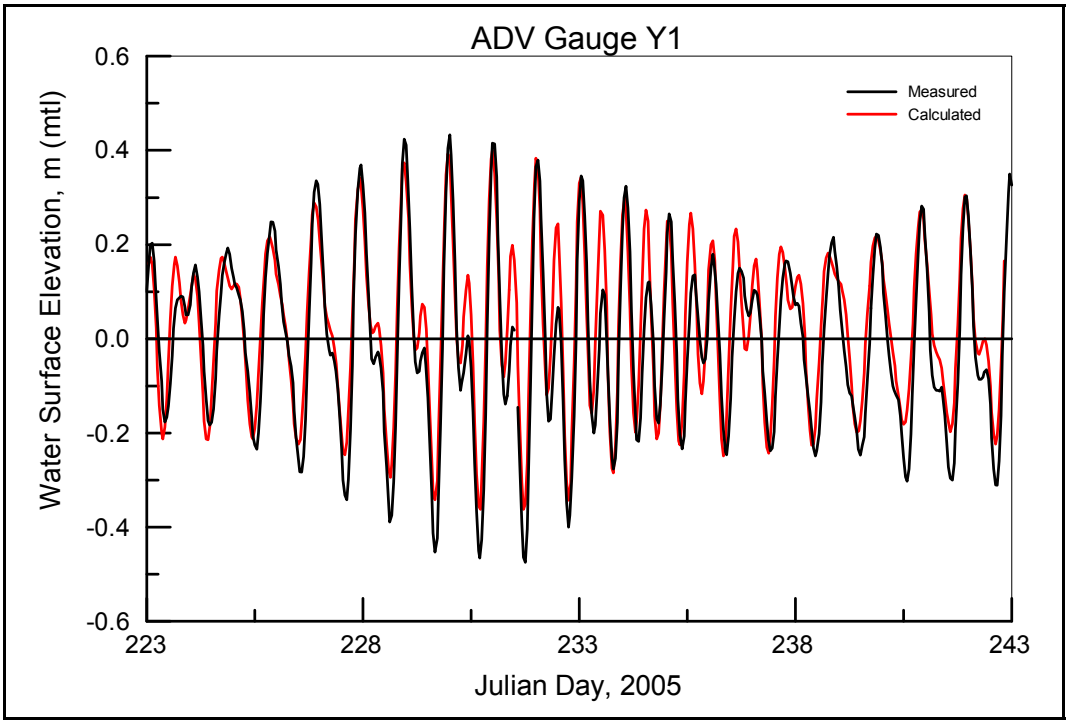

Figure 40. Water level comparison for ADV Gauge 1.

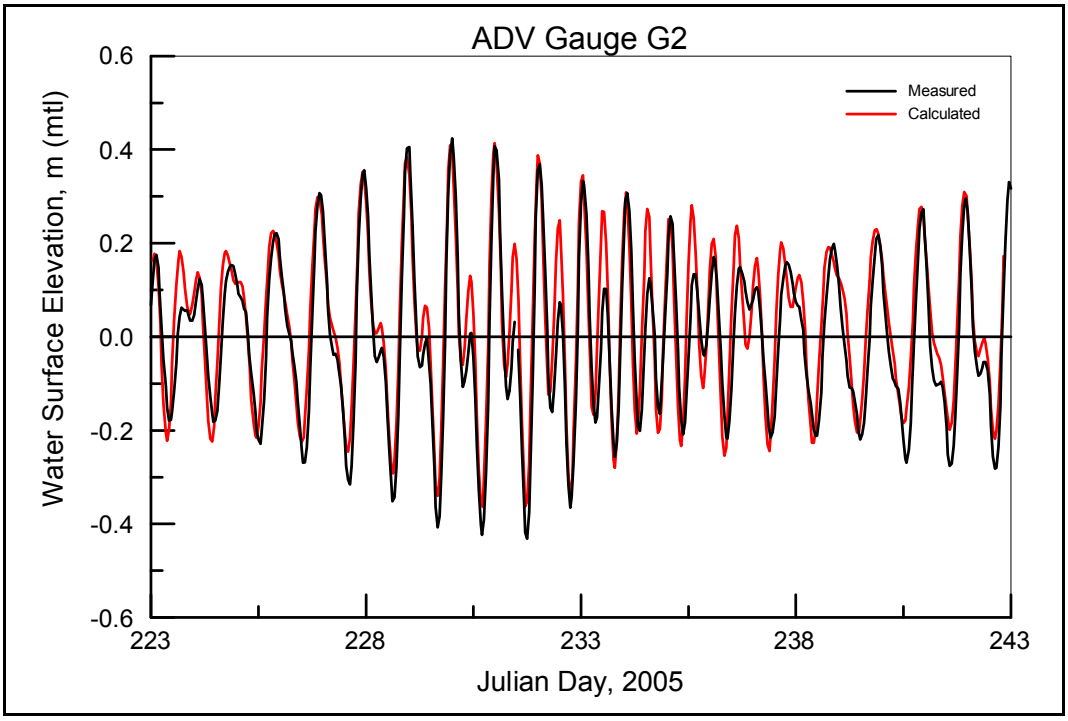

Figure 41. Water level comparison for ADV Gauge 2.

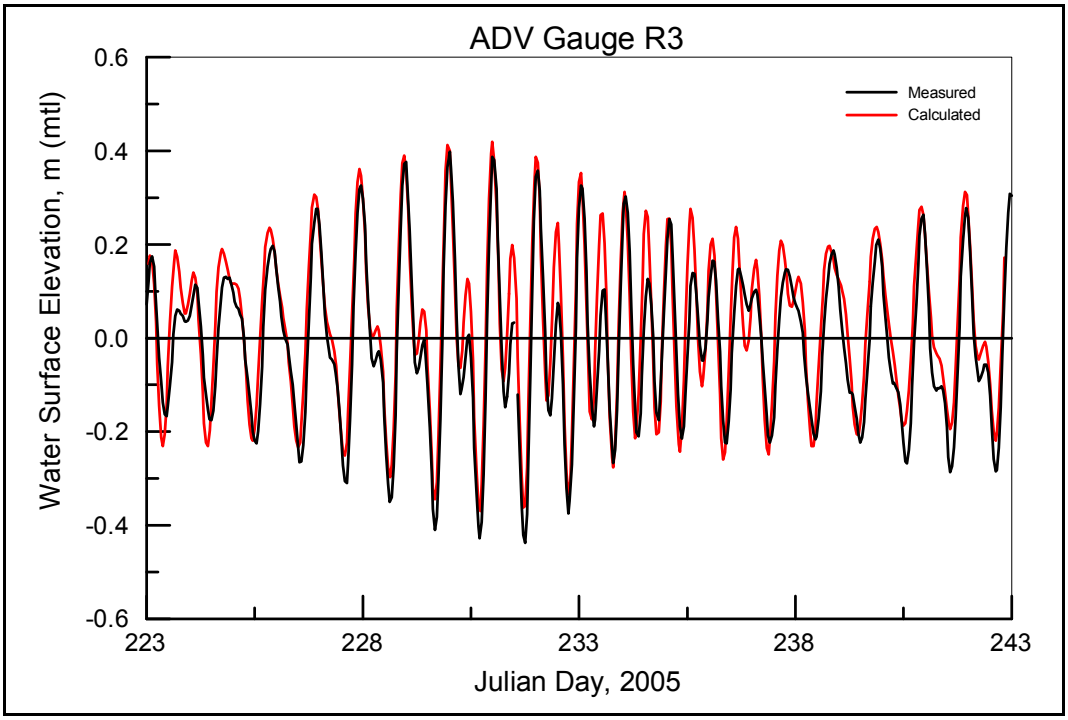

Figure 42. Water level comparison for ADV Gauge 3.

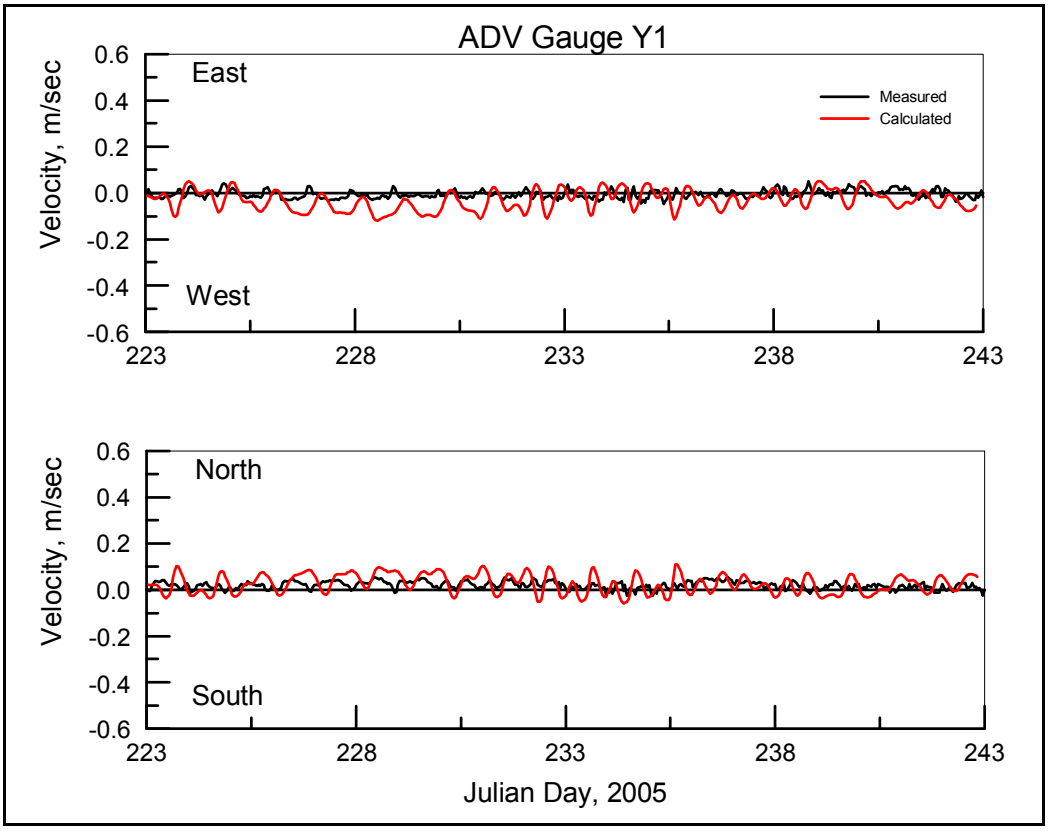

Figure 43. Velocity comparison for ADV Gauge 1.

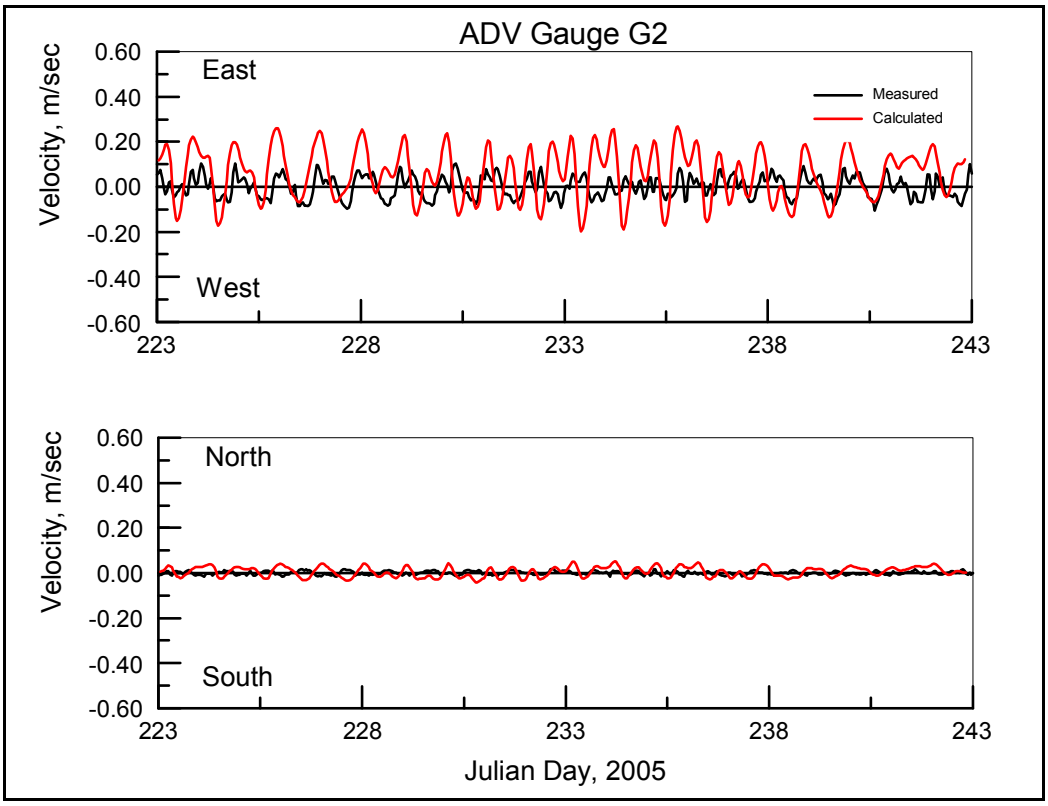

Figure 44. Velocity comparison for ADV Gauge 2.

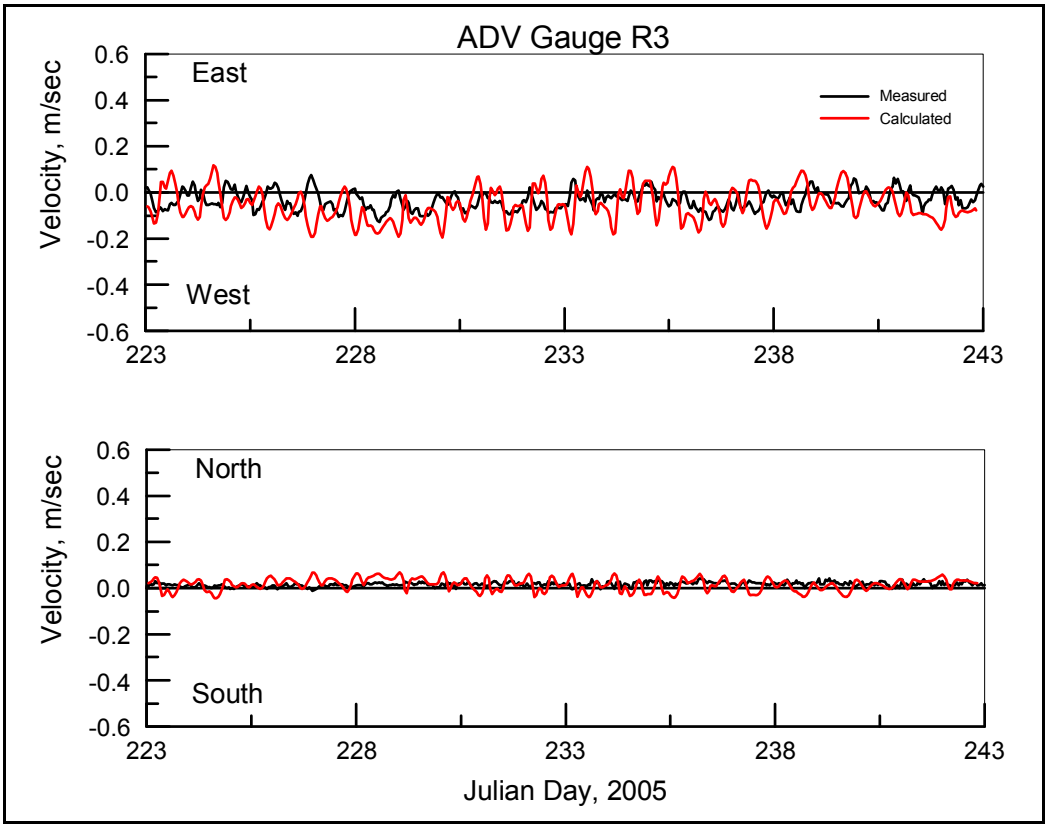

Figure 45. Velocity comparison for ADV Gauge 3.

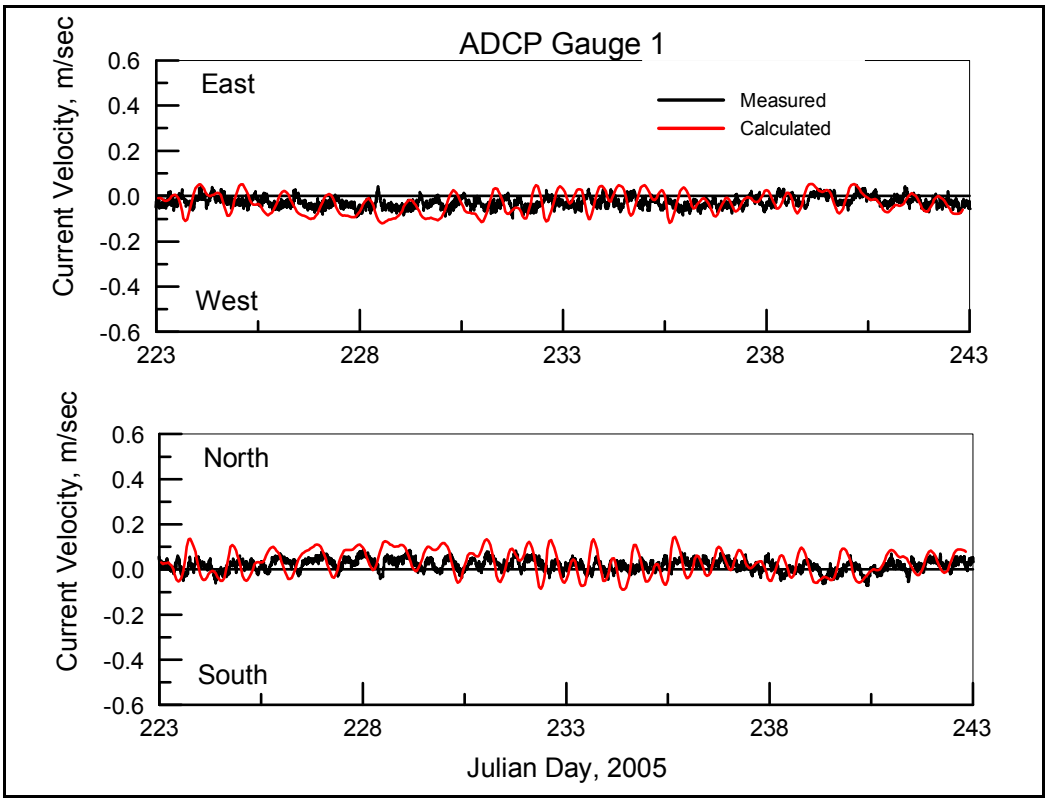

Figure 46. Velocity comparison for ADCP Gauge 1.

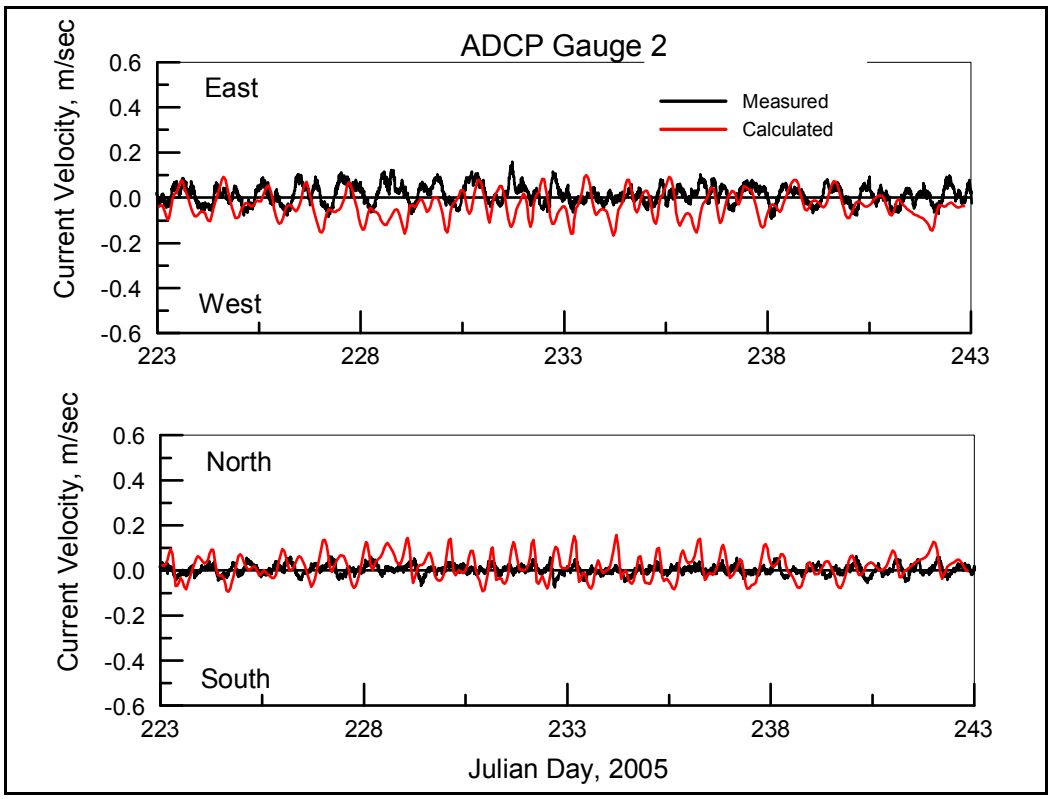

Figure 47. Velocity comparison for ADCP Gauge 2.

4 Summary

The purpose of the study was to provide POH with validated hydrodynamic and wave models for the project site. POH could then apply the models with various forcing conditions to develop a better understanding of nearshore circulation and sediment transport potential in the region and determine the likelihood of accretional and erosional areas within the model domain. The nearshore circulation study included six technical tasks: data collection/assessment, finite-element and finite-difference grid development, development of model forcing conditions, model validation, model simulations, and simulation analysis.

Wave, current, and water level data were collected in the field for a 1-month period with ADCP and ADV instruments. In addition, drogues were deployed on the 2 days that the ADCP/ADV were deployed and retrieved. Wave heights during the deployment period ranged from 0.12 to 0.69 m and were generally from the northeast direction, currents measured at the ADV and ADCP locations were small (generally less than 10 cm/sec), and water level ranged from +0.4 to -0.4 m, mtl. The drogue deployment provided general current trends for the two deployments.

A two-dimensional (depth-averaged) version of the hydrodynamic model (ADCIRC) was applied in this study. The ADCIRC modeling component for this study required grid development, validation of the bathymetric grid to known tidal constituents and wind forcing for April 2001, and comparison of the bathymetric grid forced with known tidal constituents, wind, and waves to measurements for the field data collection time period. The ADCIRC grid was developed as a circular mesh, encompassing the Hawaiian Islands, but was revised to an egg-shaped mesh to avoid tidal amphidromes in the Pacific Ocean.

For the initial model validation, ADCIRC results were compared with two NOAA gauges on the eastern half of the island of Oahu. The calculated water levels from the ADCIRC simulation of the April 2001 period compared relatively well in range and phase with the NOAA gauge measurements considering the locations of the gauges were well outside high-resolution sections of the grid in the project area. Since these gauges were outside the project area and in less resolved locations, another validation

was performed by simulating the field data collection time period and comparing model results to field data collected, specifically for this project, in the study area. Calculated water levels compared well in range and phase to measurements, but underestimated some lower peaks while overestimating some higher peaks. This may have been caused by localized interaction of the tides with the reefs surrounding the gauge locations. Current velocity data from the three ADV gauges and two ADCP gauges were extremely small during the overlapping deployment time period – generally less than 10 cm/sec. Velocities calculated at these locations from the ADCIRC circulation model were not expected to compare well to the measurements; however, the range of velocity model results is within one order of magnitude and generally very close. The application and validation of ADCIRC for the SEO study provides POH with the capability of simulating circulation in the study area for any required time period.

The purpose of applying nearshore wave transformation models such as STWAVE is to describe quantitatively the evolution of wave parameters from the offshore to the nearshore where nearshore wave information is required for the design of coastal engineering projects. STWAVE has been applied to numerous sites, and this project has the necessity of simulating wave transformation over a reef. Development of a bottom friction capability in STWAVE was completed for application to the extensive reefs in the SEO study area. Application of STWAVE for this project required development of a computational grid to simulate wave propagation, verification of calculated waves by comparison to measurements, and generation of a wave climate.

For demonstration of the wave climate development technique, nearshore conditions at a point in Waimanalo Bay were extracted from the STWAVE model results for each of the 134 simulations. A transformation correlation between the offshore and nearshore condition was then determined for each simulation. By applying the appropriate transfer function to each wave condition in the 2000–2004 offshore time series at Station 098, a long-term (2000–2004) nearshore time series was generated. The nearshore time series demonstrates that there is a reduction in wave height from the offshore location to the nearshore location, landward of the extensive reef system, as expected. The time series, however, appeared generally contained or banded between the 1.25 and 2.25 m wave height bins that were selected to represent the overall wave climate. In order to capture the nearshore transformation time series more precisely and to

include all wave conditions occurring in the time series, the range and refinement of the wave conditions simulated was expanded to 1274 wave conditions. The refined nearshore time series generated from analysis of these simulations shows a more realistic undulation in the nearshore wave height time series.

Development of a bottom friction capability in STWAVE was completed for application to the extensive reefs in the SEO study area. Based on existing literature, values of the JONSWAP bottom friction applied for coral reefs range from 0.04 to 0.12 m/sec. A single friction value can be applied to the entire STWAVE domain, or a range of friction values can be applied on a spatially varying basis. As an example, the 134 wave conditions simulated in the initial climate development were repeated with the revised STWAVE, applying a bottom friction coefficient typical for reefs of 0.05. With the inclusion of bottom friction, wave height at the nearshore location ranged from 18–38% of the previous results without bottom friction. On average, the wave height is 26% of the frictionless value at the selected location. The total wave spectrum refracts less with the inclusion of bottom friction, likely due to the dissipation of low-frequency energy. As another example, for each of the 1274 selected wave conditions simulated for the revised wave climate, wave transformation *including bottom friction* was simulated by applying STWAVE over the project domain for each of the 1274 wave spectra. The constant 0.05 value of bottom friction reduced nearshore wave heights by approximately 73% compared to wave heights without bottom friction.

The extended domain STWAVE grid was applied in the model validation process for the August 2005 model validation time period. Initially, a constant bottom friction value was applied to each cell of the STWAVE domain. Several simulations with different constant JONSWAP bottom friction values ranging from 0.04 to 0.12 were made to examine the range of response (wave height) at the gauge locations. Bottom friction reduced wave height at the ADV1 location by 64% for a bottom friction value of 0.04 (wave height is 36% of the offshore wave height), by 71–76% for a bottom friction value of 0.05 (wave height is 24–29% of the offshore wave height), and by 93% for a bottom friction value of 0.12 (wave height is 7% of the offshore wave height). The range of response indicates the importance of selecting the appropriate bottom friction value to represent the reefs in the study area.

In the validation simulation, a variable bottom friction field was utilized. Overall, all three measurement locations experience low wave energy relative to the offshore waves. The STWAVE model captures the large reduction in wave height from the offshore location to the three nearshore locations. The coral reefs in this region are described as "mushroom fields." Some areas of the reef are more solid and some areas have gaps and holes in the reef. Without detailed knowledge of the contiguous/noncontiguous areas of the reef, an educated attempt was made to represent the variations in the reef. The center section of the reef was given a smaller friction coefficient and the southern portion of the reef was given a larger coefficient. These adjusted values were selected based upon the under/overprediction of wave height at ADV2 and ADV3, respectively, in the simulation with a constant reef coefficient. Tidal fluctuation was also included in these simulations. With a variable bottom friction coefficient to represent variability in the reef structure, model results compare extremely well with the data at all three gauge locations with both the Manning and the JONSWAP friction formulations. The MPI values are 0.948 to 0.970 for the Manning simulations and 0.951 to 0.953 for the JONSWAP simulations. The magnitude and trend as well as the tidal fluctuation exhibited by the data were all captured by the model.

Lessons learned from this study include:

1. The technique of developing a nearshore wave climate by applying STWAVE for a large number (range) of offshore wave conditions provides a permanent "look up" table of nearshore wave conditions at any location in the computational domain and can be applied to any time period for which offshore data are available, provided that bathymetric conditions within the model domain remain similar. Note that the creation of a nearshore wave climate was applied to generate a nearshore time series for the 2000–2004 time period, and POH is applying the database-generated time series to develop sediment transport potential estimates in the project area. A follow-on study extended the time series through 2005 and expanded to 10 save point locations;
2. From the ADCIRC validation for the deployment time period and also from examination of the retrieved deployment data, it was concluded that the tidal and wave-induced currents in the project area are small and not sufficient to significantly transport sediment. A follow-on study is being conducted to examine simulation of higher energy (storm) conditions,

which may produce waves and currents that are strong enough to transport sediment; and

3. An improved model capability was developed for this study. Bottom friction was added to STWAVE to simulate wave transformation over reefs. It was shown that bottom friction is extremely important and has a pronounced effect on modeling transformation over reefs, decreasing wave heights from the without-friction condition by 71–76% for a constant JONSWAP bottom friction value of 0.05. Simulation of the transformation process over reefs could be improved further by including wave ponding, applying a more detailed breaking formulation such as Battjes and Janssen (1978), and implementing a coupling scheme between ADCIRC and STWAVE. In addition, field data collected for this project can be further analyzed to examine spectral energy dissipation from gauge location to gauge location and nonlinear interactions. These research topics may be examined in future STWAVE model development and application.

CHL assisted POH by documenting the methodologies and procedures used in this study and providing consultation in executing simulations and analyzing simulation results. STWAVE and ADCIRC working sessions have been conducted at POH and the completed modeling system was transferred to POH within the SMS framework.

5 References

Battjes, J. A., and J. P. F. M. Janssen. 1978. Energy loss and set-up due to breaking of random waves. *Proceedings, 16th International Conference on Coastal Engineering*. 569–587.

Bouws, E., and G. J. Komen. 1983. On the balance between growth and dissipation in extreme, depth limited wind-sea in the southern North Sea. *Journal of Physical Oceanography* 13:1653–1658.

Egbert, G., A. Bennett, and M. Foreman. 1994. TOPEX/Poseidon tides estimated using a global inverse model. *Journal of Geophysical Research* 99(C12): 24821–24852.

Guza, R. T., and E. B. Thornton. 1980. Local and shoaled comparisons of sea surface elevations, pressures, and velocities. *Journal of Geophysical Research* 85(C3):1524–1530.

Hardy, T. A. 1993. *The attenuation of spectral transformation of wind waves on a coral reef*. Townsville, Queensland, Australia: James Cook University of North Queensland.

Hasselmann, K., T. P. Barnett, E. Bouws, H. Carlson, D. E. Cartwright, K. Enke, J. A. Ewing, H. Gienapp, D. E. Hasselmann, P. Kruseman, A. Meerbrug, P. Muller, D. J. Olbers, K. Richter, W. Sell, and H. Walden. 1973. Measurements of wind-wave growth and swell decay during the Joint North Sea Wave Project (JONSWAP). *Dtsch. Hydrogr. Z.* A80(12), 95 pp.

Hearn, C. J. 1999. Wave-breaking hydrodynamics within coral reef systems and the effect of changing relative sea level. *Journal of Geophysical Research* 104(C12):30007–30019.

Holthuijsen, L. H. 2007. *Waves in ocean and coastal waters*. Cambridge: Cambridge University Press.

Kraus, N. C. 2006. *Mid-Bay Islands hydrodynamics and sedimentation modeling study, Chesapeake Bay*. ERDC/CHL TR-06-10. Vicksburg, MS: U.S. Army Engineer Research and Development Center.

Kraus, N. C., and H. T. Arden. 2003. *North jetty performance and entrance navigation channel maintenance, Grays Harbor, Washington; Vol 1: Main Text*. ERDC/CHL TR-03-12. Vicksburg, MS: U.S. Army Engineer Research and Development Center.

LeProvost, C. M., L. Genco, F. Lyard, P. Vincent, and P. Canceil. 1994. Spectroscopy of the world ocean tides from a finite element hydrodynamical model. *Journal of Geophysical Research* 99(C12):24777–24797.

Lowe, R. J., J. L. Falter, M. D. Bandet, G. Pawlak, M. J. Atkinson, S. G. Monismith, and J. R. Koseff. 2005. Spectral wave dissipation over a barrier reef. *Journal of Geophysical Research* 110(C04001).

Luettich, R. A., Jr., J. J. Westerink, and N. W. Scheffner. 1992. *ADCIRC: An advanced three-dimensional circulation model for shelves coasts and estuaries, report 1: theory and methodology of ADCIRC-2DDI and ADCIRC-3DL*. Dredging Research Program Technical Report DRP-92-6. Vicksburg, MS: U.S. Army Engineer Waterways Experiment Station.

Padilla-Hernández, R., and J. Monbaliu. 2001. Energy balance of wind waves as a function of the bottom friction formulation. *Coast. Eng*. 43(2):131–148.

Resio, D. T. 1988. A steady-state wave model for coastal applications. *Proceedings of the 21st Coastal Engineering Conference*, ASCE, 929–940.

Sea Engineering, Inc. 2008 (Draft). Lanikai Beach Restoration Study Conceptual Design Report. Prepared for: USACE, Honolulu District by Sea Engineering, Inc. and Group 70 International.

Smith, J. M. 2000. Benchmark tests of STWAVE. *Proceedings, 6th International Workshop on Wave Hindcasting and Forecasting*, 169–379.

Smith, J. M., A. R. Sherlock, and D. T. Resio. 2001. *STWAVE: Steady-state spectral wave model user's manual for STWAVE, Version 3.0*. ERDC/CHL SR-01-1. Vicksburg, MS: U.S. Army Engineer Research and Development Center.

U.S. Army Corps of Engineers (USACE). 2006. Louisiana Coastal Protection and Restoration (LACPR) Preliminary Technical Report to United States Congress.

U.S. Army Corps of Engineers (USACE), Mobile District. 2008. Mississippi Coastal Improvements Program (MSCIP) Comprehensive Plan and Integrated Programmatic Environmental Impact Statement. Draft peer review plan, 498 p. plus Appendixes.

Wozencraft, J. M., and J. L. Irish. 2000. Airborne lidar surveys and regional sediment management. *Proceedings, 2000 EARSeL: Lidar Remote Sensing of Land and Sea, EARSeL*. Dresden, Germany.

REPORT DOCUMENTATION PAGE

Form Approved
OMB No. 0704-0188

1. REPORT DATE *(DD-MM-YYYY)*	2. REPORT TYPE	3. DATES COVERED *(From - To)*
July 2008	Final report	

4. TITLE AND SUBTITLE

Southeast Oahu Coastal Hydrodynamic Modeling with ADCIRC and STWAVE

5a. CONTRACT NUMBER

5b. GRANT NUMBER

5c. PROGRAM ELEMENT NUMBER

6. AUTHOR(S)

Mary A. Cialone, Mitchell E. Brown, Jane M. Smith, and Kent K. Hathaway

5d. PROJECT NUMBER

5e. TASK NUMBER

5f. WORK UNIT NUMBER

7. PERFORMING ORGANIZATION NAME(S) AND ADDRESS(ES)

U.S. Army Engineer Research and Development Center
Coastal and Hydraulics Laboratory
3909 Halls Ferry Road
Vicksburg, MS 39180-6199

8. PERFORMING ORGANIZATION REPORT NUMBER

ERDC/CHL TR-08-9

9. SPONSORING / MONITORING AGENCY NAME(S) AND ADDRESS(ES)

U.S. Army Engineer District, Honolulu
Building 230
Fort Shafter, HI 96858-5440

10. SPONSOR/MONITOR'S ACRONYM(S)

11. SPONSOR/MONITOR'S REPORT NUMBER(S)

12. DISTRIBUTION / AVAILABILITY STATEMENT

Approved for public release; distribution is unlimited.

13. SUPPLEMENTARY NOTES

14. ABSTRACT

This study provides the Honolulu District (POH) with numerical modeling tools for understanding nearshore circulation and sediment transport for Southeast Oahu (SEO). Circulation and wave models are developed and validated for this region and can be applied to assess sediment transport potential for various forcing conditions and to determine the likelihood of accretional and erosional areas within the model domain.

Application of a wave model includes the generation of a wave climate. In the wave climate development technique, near-shore conditions are extracted from the wave model results for each simulation. A transformation correlation between the offshore and nearshore condition is then determined for each simulation. By applying the appropriate transfer function to each wave condition in the offshore time series, a long-term nearshore time series is generated. The nearshore time series demon-strates that there is a reduction in wave height from the offshore location to the nearshore location, landward of the extensive reef system as expected. The technique of developing a nearshore wave climate by applying the wave model for a range of offshore wave conditions provides a permanent "look up" table of nearshore wave conditions at any location in the

(Continued)

15. SUBJECT TERMS

ADCIRC
Circulation model
Hydrodynamic model
Oahu, HI
STWAVE
Two-dimensional model
Wave model

16. SECURITY CLASSIFICATION OF:			17. LIMITATION OF ABSTRACT	18. NUMBER OF PAGES	19a. NAME OF RESPONSIBLE PERSON
a. REPORT	b. ABSTRACT	c. THIS PAGE			19b. TELEPHONE NUMBER *(include area code)*
UNCLASSIFIED	UNCLASSIFIED	UNCLASSIFIED		60	

14. ABSTRACT (Concluded)

computational domain and can be applied to any time period for which offshore data are available, provided that bathymetric conditions within the model domain remain similar. POH is applying the database-generated time series to develop sediment transport potential estimates in the project area.

Development of a bottom friction capability in the wave model was completed for application to the extensive reefs in the SEO study area. It is shown that bottom friction is extremely important and has a pronounced effect on modeling transformation over reefs, decreasing wave heights from the without-friction condition by 71-76% for a constant JONSWAP bottom friction value of 0.05.